1-2014

East-derived Strata in the Methow Basin Record Rapid Mid-Cretaceous Uplift of the Southern Coast Mountains Batholith

Kathleen D. Surpless
Trinity University, ksurples@trinity.edu

Zachary T. Sickmann
Trinity University, zsickman@trinity.edu

Trevor Koplitz
Trinity University, tkoplitz@trinity.edu

NRC Research Press

ARTICLE

East-derived strata in the Methow basin record rapid mid-Cretaceous uplift of the southern Coast Mountains batholith[1]

Kathleen D. Surpless, Zachary T. Sickmann, and Trevor A. Koplitz

Abstract: The Jurassic–Cretaceous Methow basin of northern Washington State and southern British Columbia forms an overlap sequence linking several small tectonostratigraphic terranes. Sandstone petrography, sandstone and mudrock geochemistry, and detrital zircon U–Pb age and Hf analysis of mid-Cretaceous, east-derived Methow strata together document a remarkably uniform provenance signature that suggests proximal, abundant, and unchanging sediment sources throughout deposition. The eastern belt of the Coast Mountains batholith, intruded into Stikine and related inboard terranes of the Intermontane superterrane, along with Jurassic and Cretaceous plutons of the westernmost Okanogan Range, provide the best match to the provenance signature of east-derived sediment in the Methow basin during the mid-Cretaceous. Furthermore, the Cretaceous and Jurassic plutons of the eastern Coast Mountains batholith and western Okanogan Range were rapidly uplifted to provide the substantial thickness of sediment in the Methow basin, and they must have acted as a topographic barrier that effectively prevented sediment derived from the continental interior from reaching the basin. This uplift of a proximal eastern source occurred during regional late Early Cretaceous sinistral transpression and resulted in subsidence of the Methow trough and rapid deposition of east-derived strata in the Methow basin. Because Methow sediment sources apparently did not include the North American interior, the extent of post-depositional large-scale translation relative to the North American craton of the Methow basin with its proximal, eastern sources cannot be unequivocally determined.

Résumé : Le bassin de Methow (Jurassique–Crétacé) du nord de l'État de Washington et du sud de la Colombie-Britannique forme une séquence de chevauchement reliant plusieurs petits terranes tectonostratigraphiques. La pétrographie des grès, la géochimie des grès et des pélites ainsi que les âges déterminés par U–Pb sur des zircons détritiques et des analyses Hf des strates de Methow provenant de l'est (Crétacé moyen) documentent ensemble une signature de provenance remarquablement uniforme, suggérant des sédiments de sources proximales, abondantes et inchangées durant toute la déposition. La ceinture est du batholite de la Chaîne côtière, introduite dans le terrane de Stikine et d'autres terranes intérieurs reliés du superterrane intermontagneux, et les plutons datant du Jurassique et du Crétacé de la partie la plus à l'ouest du chaînon Okanogan, fournissent la meilleure concordance pour une signature de provenance de sédiments de l'est vers le bassin de Methow au Crétacé moyen. De plus, les plutons datant du Crétacé et du Jurassique du batholite de l'est de la chaîne Côtière et de l'ouest du chaînon Okanagan ont été soulevés rapidement, fournissant l'importante épaisseur de sédiments dans le bassin de Methow, et ils ont dû agir de barrière topographique qui a effectivement empêché les sédiments provenant de l'intérieur du continent d'atteindre le bassin. Ce soulèvement d'une source proximale à l'est a eu lieu durant une transpression senestre régionale, à la fin du Crétacé précoce, et a conduit à la subsidence de la fosse de Methow et à la déposition rapide de strates provenant de l'est dans le bassin de Methow. Puisque les sources des sédiments du bassin de Methow n'incluaient apparemment pas l'intérieur de l'Amérique du Nord, l'étendue de la translation post-déposition à grande échelle du bassin de Methow avec ses sources proximales de l'est, par rapport au craton de l'Amérique du Nord, ne peut pas être déterminée de manière catégorique. [Traduit par la Rédaction]

Introduction

Unraveling the tectonic history of amalgamation and subsequent accretion, deformation, and coast-parallel translation of terranes within the North American Cordillera is at the core of longstanding questions and controversy regarding the Mesozoic and younger Cordillera (e.g., Haggart et al. 2006). Moreover, magmatic arcs in different regions of the North American Cordillera have undergone episodes of magmatic flux, uplift, and exhumation that varied in their timing, rate, and magnitude (e.g., Ducea 2001; Kimbrough et al. 2001; Gehrels et al. 2009). Examining the stratigraphy of sedimentary basins that received detritus from these uplifted and dissected arcs provides crucial information for better understanding active arc processes and Cordilleran tectonic events.

The Jurassic–Cretaceous Methow–Tyaughton basin, currently located in northern Washington State and southern British Columbia (Fig. 1), was deposited during suturing of the Insular and Intermontane superterranes (Monger et al. 1982; Armstrong 1988; Thorkelson and Smith 1989; Garver 1992). Previous research focused on detrital zircon analysis of east-derived sediment that filled the Methow basin during and following Insular superterrane accretion, and concluded that the Methow detrital zircon age spectra match well with ages of plutonic source regions in the southern Canadian Cordillera, suggesting only minor post-accretion

Received 2 August 2013. Accepted 15 November 2013.

Paper handled by Associate Editor Graham Andrews.

K.D. Surpless, Z.T. Sickmann,* and T.A. Koplitz.† Trinity University, One Trinity Place, San Antonio, TX 78212, USA.

Corresponding author: Kathleen D. Surpless (e-mail: ksurples@trinity.edu).

*Current address: Department of Geological and Environmental Sciences, 450 Serra Mall, Building 320, Stanford, CA 94305-2115, USA.

†Current address: 2902 Calhoun Street, New Orleans, LA 70118, USA.

[1]This article is one of a series of papers published in this Special Issue on the theme of *New insights in Cordilleran Intermontane geoscience (Part 2).*

Fig. 1. (A) Geologic map of the southern Methow block showing units and structures discussed in the text as well as sample sites; white numbers in sample sites correspond to sample location numbers provided in Table 1. Map adapted from Enkin et al. (2002) and McGroder et al. (1990). (B) Regional geologic map of the southern Canadian Cordillera showing major structural features and terranes (from Enkin et al. 2002). The northern and southern blocks of the Methow terrane are shown in stippled grey pattern. (C) Overview map of the Canadian Cordillera showing the distribution of tectonic belts (from Enkin et al. 2002). The area of B is outlined in black.

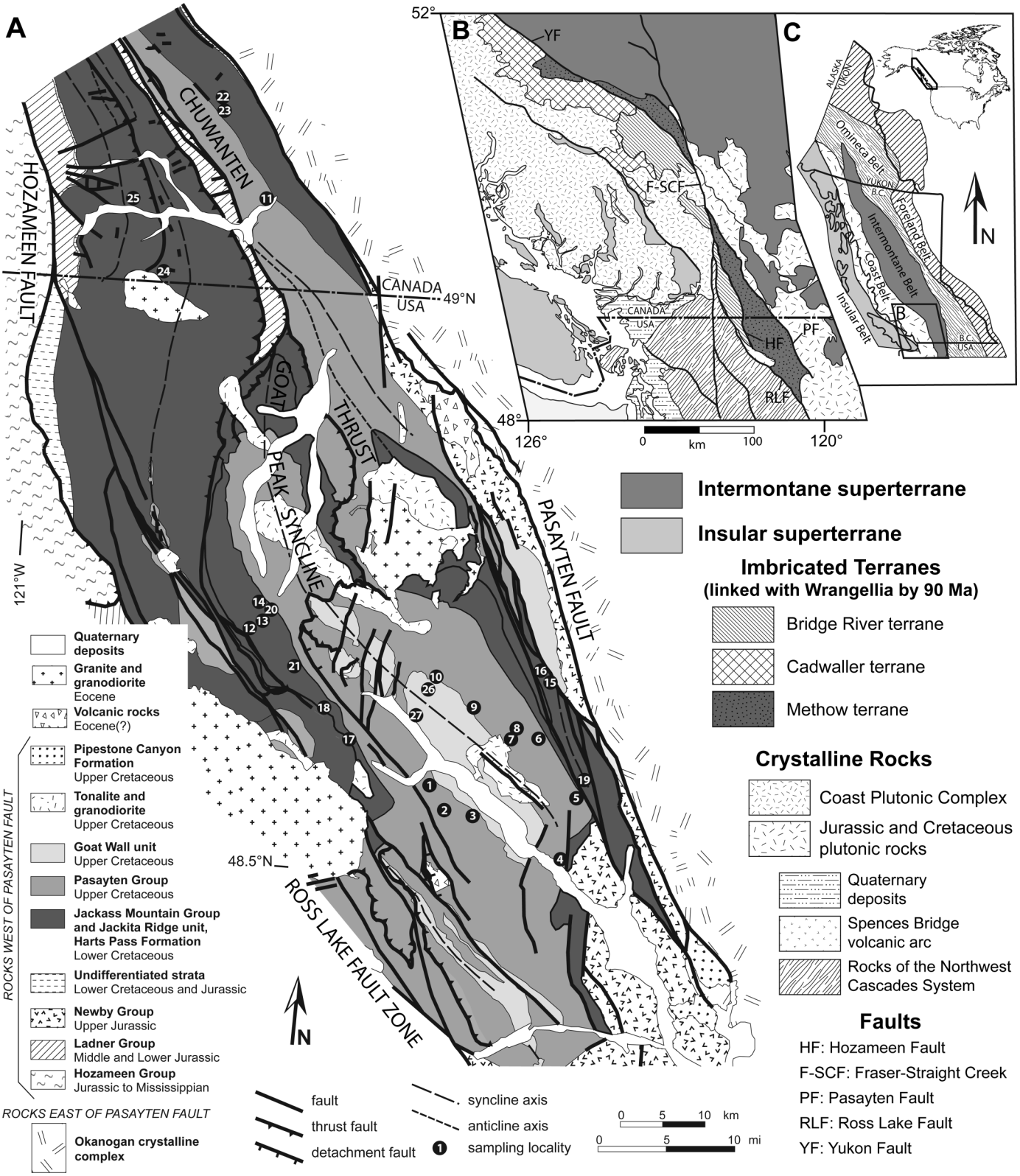

dextral translation of the Insular superterrane to its present location (DeGraaff-Surpless et al. 2003). In this paper, we present new detailed provenance data from the east-derived Harts Pass and Winthrop formations and the overlying Goat Wall unit within the Methow basin to document temporal and spatial changes in source-basin evolution through mid-Cretaceous time.

Sandstone petrography, sandstone and mudrock geochemistry, and new detrital zircon U–Pb age and Hf analysis of east-derived Methow strata together document a remarkably uniform provenance signature that suggests proximal, abundant, and unchanging sediment sources throughout deposition. Consistent with previous provenance interpretations (DeGraaff-Surpless et al. 2003), the eastern belt of the Coast Mountains batholith (cf. Gehrels et al. 2009) and plutons of the westernmost Okanogan Range (Petö and Armstrong 1976) provide the best match to the provenance signature of east-derived sediment in the Methow basin during the mid-Cretaceous. Furthermore, mid-Cretaceous subsidence of the Methow basin occurred with rapid uplift of the Jurassic and Cretaceous plutons of the eastern Coast Mountains batholith and westernmost Okanogan Range, permitting deposition of a substantial thickness of east-derived sediment in the Methow basin. The uplifted Jurassic and Cretaceous magmatic arc acted as a topographic barrier that effectively prevented sediment derived from the continental interior from reaching the basin. Late Early Cretaceous regional transpression resulted in subsidence of the Methow trough and uplift of terranes immediately east of the basin.

Although consensus has not yet emerged regarding the complete history of accretion, magmatism, and terrane translation (e.g., Butler et al. 2001; Haggart et al. 2006), several paleotectonic models have been proposed that juxtapose terranes and predict stratigraphic correlation between currently separate sedimentary basins (e.g., Umhoefer and Blakey 2006; Wyld et al. 2006; Dorsey and Lenegan 2007). For example, Wyld et al. (2006) suggest that the Methow basin may have formed the northern continuation of a combined Hornbrook–Ochoco basin, and Umhoefer and Blakey (2006) suggest that the Methow basin may have been located outboard of the Great Valley Group during mid-Cretaceous deposition. The detailed provenance signature of mid-Cretaceous strata in the Methow basin we present here is distinct from that of the Hornbrook and Ochoco basins, as well as the Great Valley Group. In fact, our detailed Methow basin provenance signature does not match well with any coeval sedimentary basins or potential sources to the south in the US and Mexican Cordillera. However, because Methow sediment sources apparently did not include the North American interior, the extent of post-depositional large-scale translation relative to the North American craton of the Methow basin, together with its proximal magmatic arc sources, cannot be unequivocally determined.

The Methow basin

Regional framework

Jurassic and Cretaceous strata that unconformably overlie the Lower Triassic Spider Peak Formation (Ray 1990) comprise the Methow terrane, which consists of a northern and southern block separated by Late Cretaceous to Paleogene dextral translation on the Fraser – Straight Creek fault system (Fig. 1B; Monger 1970; Kleinspehn 1982; Umhoefer and Schiarizza 1996). Similar Jurassic and Lower Cretaceous strata unconformably deposited on the Bridge River and Cadwallader terranes are considered part of the Tyaughton basin, an adjacent basin that was linked with the Methow basin to form the continuous Methow–Tyaughton system by Late Cretaceous time (Garver 1989, 1992), but may have been associated by as early as Middle Jurassic time (Mahoney 1994). The Cretaceous Methow–Tyaughton rocks are located between the Insular and Intermontane superterranes (Fig. 1B; Kleinspehn 1985; Garver 1992; Garver and Brandon 1994; Haugerud et al. 1996). East of the Methow–Tyaughton system are Jurassic and Cretaceous plutons of the Okanogan Range and the eastern belt of the Coast Mountains batholith (cf. Gehrels et al. 2009), as well as the amalgamated terranes of the Intermontane superterrane (Quesnel and Cache Creek terranes) and the Omineca Belt (Fig. 1C). The southern Methow block spans the Canadian–USA border, and is bordered by the Pasayten fault to the east and the Hozameen — Straight Creek fault system and the Ross Lake fault to the west (Fig. 1A).

Tectonic history

Upper Paleozoic and Lower Mesozoic ribbon chert and greenstone of the Hozameen and Bridge River Groups form the basement of the Cretaceous Methow basin, and have been interpreted as an accretionary complex thrust onto the continent during subduction (Kleinspehn 1985; Garver 1992; Garver and Brandon 1994; Garver and Scott 1995). Lower Mesozoic volcanic and volcaniclastic rocks were deposited in the Methow basin forearc associated with Early Mesozoic subduction (Tennyson and Cole 1978; Haugerud et el. 1996). Lower Cretaceous units, which include the Jackass Mountain Group and partly correlative Harts Pass Formation (Garver and Brandon 1994; Mahoney 1994; DeGraaff-Surpless et al. 2003; MacLaurin et al. 2011), are composed of terrigenous, east-derived sediment that was derived from volcanic and plutonic source rock and deposited on the older basement terranes (Kleinspehn 1985).

During mid-Cretaceous compression (Tennyson and Cole 1978) associated with the accretion of the Insular superterrane with North America (Kleinspehn 1982; Garver et al. 1988; Garver 1989, 1992), the Bridge River Complex – Hozameen Group was uplifted either through transpressive wrench-faulting (Trexler and Bourgeois 1985), or as an accretionary wedge developed along western North America (Garver and Brandon 1994; Garver and Scott 1995). The uplift of the Bridge River Complex – Hozameen Group west of the Methow basin margin provided a new western sediment source beginning in middle Albian time that is represented in the west-derived Little Jack and Jackita Ridge units (Haugerud et al 1996) and the Virginian Ridge Formation (Trexler and Bourgeois 1985; Garver 1992; Garver and Brandon 1994). The Little Jack and Jackita Ridge units interfinger with the east-derived Harts Pass Formation, and the Virginian Ridge Formation interfingers with the east-derived Winthrop Formation. The Virginian Ridge and Winthrop formations are overlain by the volcanic-rich Goat Wall unit (formerly Midnight Peak Formation; Enkin et al 2002), recording the ultimate filling of the basin (Kiessling and Mahoney 1997; Kiessling 1998).

Late Cretaceous and Paleogene deformation uplifted, folded, and faulted the Methow basin, resulting in intrabasinal thrust faults, local unconformities, and east-vergent folding (Tennyson and Cole 1978; Kleinspehn 1985; Garver 1992). Approximately 110 km of dextral displacement on the Fraser – Straight Creek fault occurred during Late Cretaceous to middle Paleogene time (Kleinspehn 1985), with separation of the northern and southern blocks of the Methow terrane occurring between ca. 44 and 34 Ma (Enkin et al. 2002). The extent of Cretaceous to early Paleogene displacement on the Pasayten fault is more controversial (e.g., Lawrence 1978; Butler et al. 1989; Hurlow 1993; Wynne et al. 1995; Wyld et al. 2006). The Pasayten fault has been proposed as the locus for large-scale dextral translation; values of displacement on the Pasayten fault range from <1000 km (e.g., Butler et al. 1989; Kodama and Ward 2001) to >3000 km of displacement (e.g., Wynne et al. 1995; Irving et al. 1996; Ward et al. 1997).

East-derived strata

The upper Jackass Mountain Group in southern British Columbia and correlative Harts Pass Formation in northern Washington State (Figs. 1A, 2) formed in the waning stages of an Early Cretaceous open marine environment (Kleinspehn 1985), with deposition of the west-derived Little Jack and Jackita Ridge units indicating emergence of a western source during Albian time (Haugerud et al. 1996). The Jackass Mountain Group is Hauterivian

Fig. 2. Schematic stratigraphy of the Methow basin, modified from Enkin et al. (2002) and DeGraaff-Surpless et al. (2003).

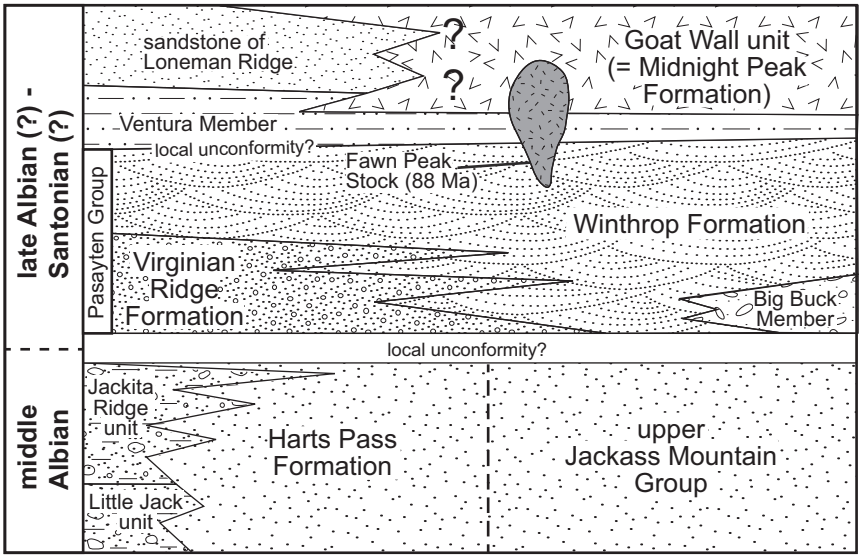

to Albian in age and contains volcanic-rich lithic wacke, felspathic wacke, and boulder conglomerate (Kleinspehn 1985; MacLaurin et al. 2011). Paleocurrent indicators, such as cross-laminae, along with upward-fining sequences and grading patterns suggest that Jackass Mountain sedimentation occurred as periodic mass flows and turbidity currents within a submarine fan system (Coates 1974; Tennyson and Cole 1978; Kleinspehn 1985). Although plant debris occurs in the Jackass Mountain Group, Kleinspehn (1982) interpreted an overall lack of fauna as indicative of sedimentation in a marine environment. Alternatively, MacLaurin et al. (2011) interpreted a large, shallow-water deltaic depositional environment for the Jackass Mountain Group in the northern Methow block, with a west-northwest–east-southeast-trending paleoshoreline.

The upper portion of the Jackass Mountain Group in Canada has been correlated with the Harts Pass Formation in Washington, and is considered Albian in age (Fig. 2; Tennyson and Cole 1978; McGroder et al. 1990; Haugerud et al. 1996). The Harts Pass Formation is up to 3200 m thick (Barksdale 1975; McGroder et al. 1990) and consists of graded sandstone and siltstone beds with high plagioclase and low potassium feldspar content (Tennyson and Cole 1978). Paleocurrent analyses of groove casts, elongate clast orientation, ripple-drift cross-laminations, and flute marks indicate westward transport of sediment in turbidity currents that formed submarine fans (Tennyson and Cole 1978). Following McGroder et al. (1990), we refer collectively to the upper Jackass Mountain Group in southernmost British Columbia and the Harts Pass Formation in northern Washington State as the Harts Pass Formation.

The Pasayten Group was deposited on the Harts Pass Formation with local unconformity, and includes the Virginian Ridge Formation, Winthrop Formation, and Goat Wall unit (former Midnight Peak Formation; Coates 1974; Haugerud et al. 1996; Enkin et al. 2002). The Virginian Ridge Formation is of Cenomanian(?) to Turonian age, locally contains gastropod fossils of probable Turonian age (Fig. 2; Enkin et al. 2002), and has variable thickness of 300–3400 m (Barksdale 1975; Haugerud et al. 1996; Enkin et al. 2002). The Virginian Ridge Formation has been interpreted as a west-derived deltaic fan system based on paleocurrent indicators, including ripple-drift cross-laminations, and eastward thinning (Tennyson and Cole 1978; Trexler and Bourgeois 1985). The Virginian Ridge Formation primarily consists of argillite, siltstone, and sandstone with some chert pebble conglomerates (Tennyson and Cole 1978; Trexler and Bourgeois 1985; Garver 1992; Haugerud et al. 1996). The typical mode given by Tennyson and Cole (1978) of $Q_{30}F_{25}L_{45}$ includes about 40% chert fragments. Because of its high chert content, the western source for the Virginian Ridge Formation has been interpreted as the uplifted Hozameen or Bridge River Group accretionary complex rocks that formed a western sediment source for the mid-Cretaceous Methow basin (Trexler and Bourgeois 1985; Garver 1992). The west-derived Virginian Ridge Formation interfingers with the largely contemporaneous, east-derived Winthrop Formation.

The up to 4000 m thick Albian to Turonian Winthrop Formation consists of primarily fluvial and deltaic deposits oriented to the south-southeast, with abundant trough cross-bedding, small cross laminations, and climbing ripples (Tennyson and Cole 1978; Trexler and Bourgeois 1985; Haugerud et al. 1996). Paleocurrent analysis on oriented wood fragments, cross-stratification foresets and trough axes documented an eastward direction of transport (Cole 1973). The age of the Winthrop Formation is based on Albian plant fossil assemblages (Miller et al. 2006), interfingering relationship with the Virginian Ridge Formation, a lower contact with the Albian Harts Pass Formation (Fig. 2; Coates 1974; Barksdale 1975), and crosscutting 88–90 Ma plutons (Haugerud et al. 1996). Bioturbation, wood fragments, and plant leaf fossils indicate that this formation was more continental in nature than the Harts Pass Formation (Kiessling and Mahoney 1997). The Winthrop Formation is compositionally similar to that of the older, east-derived, Harts Pass Formation, except for an increase in volcanic lithic fragments (Garver 1992; Kiessling 1998).

The Turonian to Coniacian Goat Wall unit is characterized by red mudstone intercalated with coarser-grained lithic wacke and conglomerate with high volcanic lithic fragment components and andesitic and pyroclastic flows (Tennyson and Cole 1978; Kiessling and Mahoney 1997). The Goat Wall unit includes red interbedded volcanogenic siltstone, sandstone, and conglomerate of the Ventura member, deposited in a braided fluvial system (Kiessling 1998) with a basal contact on the underlying Virginian Ridge and Winthrop formations that is locally an angular unconformity (Garver 1992). Garver (1992) considered conglomerate of the Ventura member west-derived due to its high chert content and similarity to the underlying Virginian Ridge Formation. McGroder et al. (1990) noted that the Ventura member conglomerate is more heterolithic than the Virginian Ridge Formation and contains clasts derived from underlying Methow basin units that include the Winthrop Formation and possibly the Harts Pass Formation. Sandstone clast sizes in the Ventura member conglomerate are largest where the angular unconformity between the Winthrop Formation and Ventura member is most pronounced (McGroder et al. 1990).

Table 1. Methow basin sample locations.

Sample	Location (Fig. 1)	Latitude	Longitude
Goat Wall unit			
11-MP-02	26	48°39.876′	120°27.056′
11-MP-04	27	48°38.279′	120°28.495′
Winthrop Formation			
98KD09	2	48°33.952′	120°25.797′
98KD10	2	48°33.914′	120°25.220′
98KD12	3	48°33.634′	120°23.577′
98KD13	3	48°33.634′	120°23.577′
98KD14	3	48°33.634′	120°23.577′
98KD15	3	48°33.634′	120°23.577′
98KD16	3	48°33.634′	120°23.577′
98KD17	3	48°33.634′	120°23.577′
11-WS-01	7	48°37.853′	120°21.689′
11-WS-02	7	48°37.919′	120°21.667′
11-WS-04	8	48°38.282′	120°21.216′
11-WS-05	6	48°38.217′	120°19.433′
11-WS-06	9	48°39.061′	120°23.915′
11-WS-07	10	48°40.547′	120°26.905′
11-WS-08	1	48°34.962′	120°27.175′
11-WS-09	1	48°34.962′	120°27.175′
11-WS-10	1	48°34.962′	120°27.175′
11-WS-11	1	48°34.962′	120°27.175′
11-WS-12	1	48°34.962′	120°27.175′
11-WS-15	4	48°31.893′	120°16.786′
11-WS-16	5	48°35.548′	120°16.493′
11-WS-17	5	48°35.548′	120°16.493′
11-WS-18	5	48°35.548′	120°16.493′
11-WS-19	5	48°35.548′	120°16.493′
11-WS-20	5	48°35.548′	120°16.493′
12-WS-04	11	49°05.339′	120°41.253′
Harts Pass Formation			
98KD04	12	48°41.865′	120°41.812′
98KD18	13	48°43.859′	120°40.431′
98KD19	13	48°43.859′	120°40.431′
98KD21	13	48°43.859′	120°40.431′
98KD25	14	48°43.870′	120°40.451′
11-HP-01	15	48°40.129′	120°18.238′
11-HP-02	16	48°42.087′	120°19.234′
11-HP-03	16	48°41.918′	120°19.191′
11-HP-04	16	48°41.940′	120°19.195′
11-HP-05	16	48°41.940′	120°19.195′
11-HP-06	17	48°36.983′	120°31.306′
11-HP-07	17	48°36.983′	120°31.306′
11-HP-08	18	48°38.460′	120°34.849′
11-HP-09	19	48°36.281′	120°16.015′
11-HP-10	20	48°43.732′	120°39.962′
11-HP-11	20	48°43.521′	120°39.794′
11-HP-12	20	48°43.521′	120°39.794′
11-HP-13	20	48°43.292′	120°40.125′
11-HP-14	20	48°43.292′	120°40.125′
11-HP-15	20	48°42.234′	120°38.743′
11-HP-16	21	48°42.234′	120°38.743′
Upper Jackass Mountain Group – Harts Pass Formation			
12-JMG-B-06	22	49°09.962′	120°46.073′
12-JMG-B-07	22	49°09.944′	120°46.138′
12-JMG-B-08	22	49°09.917′	120°46.174′
12-JMG-B-09	22	49°09.885′	120°46.255′
12-JMG-B-10	22	49°09.844′	120°46.314′
12-JMG-B-11	22	49°09.800′	120°46.455′
12-JMG-B-12	22	49°09.800′	120°46.455′
12-JMG-B-13	23	49°09.212′	120°46.076′
12-JMG-04	24	49°00.628′	120°50.148′
12-JMG-05	24	49°00.628′	120°50.148′
12-JMG-06	24	49°00.626′	120°50.115′
12-JMG-07	24	49°00.623′	120°50.062′
12-JMG-08	24	49°00.624′	120°50.025′
12-JMG-09	24	49°00.653′	120°49.955′
12-JMG-10	24	49°00.731′	120°49.911′
12-JMG-12	25	49°04.669′	120°54.505′
12-JMG-13	25	49°04.443′	120°54.659′
12-JMG-14	25	49°04.383′	120°54.678′
12-JMG-15	25	49°04.388′	120°54.741′
12-JMG-16	25	49°04.329′	120°54.776′
12-JMG-18	25	49°04.213′	120°54.478′

Provenance methods and results

Sandstone petrography: methods and results

Sandstone grains of the Harts Pass Formation and Winthrop Formation are poorly sorted and angular, ranging in size from 0.05 to 2 mm. Most thin sections were stained with sodium cobaltinitrite to improve identification of potassium feldspar grains; however, staining appeared only faintly, if at all, suggesting either a lack of potassium feldspar or poor staining procedures and making identification of potassium feldspar unreliable. Point counts were conducted using the methods of Dickinson (1970). At least 400 points were counted from 31 samples (see Table 1 for sample locations). Matrix content (including possible pseudomatrix) averages 1%, and ranges from <1% to as much as 4.5%; unidentifiable grains comprise up to 10.8% of a sample, with the sum of matrix/pseudomatrix and unidentifiable grains never exceeding 11.4% (Table 2). Although samples with >12% combined matrix/pseudomatrix and unidentifiable grains were not counted, significant alteration of feldspar grains and unstable lithic grains is apparent in almost all thin sections, perhaps resulting in undercounting of unstable grains.

Point-count data from 14 sandstone samples of the Harts Pass Formation yield average QFL values of $Q_{35}F_{65}L_1$ (Table 2). Both the QFL and QmFLt diagrams show that all Harts Pass samples reflect basement uplift provenance within the continental block provenance field of Dickinson et al. (1983; Fig. 3). Point-count data from 17 sandstone samples from the Winthrop Formation yield an average of $Q_{25}F_{47}L_{27}$ and record greater compositional variability than the Harts Pass Formation (Table 2). Winthrop Formation samples plot across basement uplift, dissected arc, and transitional arc provenance fields (Fig. 3). The samples with the fewest lithic grains (11-WS-05, 11-WS-20, and 12-WS-04) were collected from the base of the Winthrop Formation, and plot with the Harts Pass Formation samples within the basement uplift provenance field (Fig. 3). Lithic grain abundance increases above the basal Winthrop Formation, but not systematically up-section, and the most lithic-rich sample from the middle of the Winthrop Formation (98KD16, $Q_{10}F_{34}L_{57}$) plots within the transitional arc field, just outside of the undissected arc field. The majority (83%) of lithic grains in all samples is volcanic (Table 2), and up to seven metamorphic lithic grains were present in all but three samples.

Mudrock geochemistry: methods and results

Geochemical analysis can be particularly useful to detect continental influence on sediment, permit identification of minor minerals not readily apparent in petrographic analysis, and better characterize mafic components that may be underrepresented in both sandstone and detrital zircon provenance analysis (e.g., McLennan et al. 1993; LaMaskin et al. 2008). Twenty-five samples of mudrock were collected from the Harts Pass (18 samples) and Winthrop formations (seven samples; Table 1). Care was taken to collect relatively fresh samples without visible alteration. Sample chips were sent to the GeoAnalytical Lab at Washington State University, where they were ground to <30 μm powder and

Table 2. Recalculated modal point-count data for sandstone samples from the Methow basin.

		Q–F–L (%)			Qm–F–Lt (%)			Qp–Lv–Lsm (%)				
Sample No.	Total	Q	F	L	Qm	F	Lt	Qp	Lv	Lsm	Matrix (%)	Unidentified (%)
Winthrop Formation												
11-WS-05	400	0.25	0.72	0.03	0.24	0.72	0.03	0.17	0.67	0.17	0.25	0.5
11-WS-20	400	0.29	0.68	0.03	0.29	0.68	0.03	0.00	0.55	0.45	1	1.25
11-WS-04	400	0.37	0.53	0.10	0.35	0.53	0.11	0.12	0.81	0.07	0.25	0.5
11-WS-02	400	0.38	0.49	0.13	0.36	0.49	0.16	0.14	0.83	0.03	0	0
11-WS-01	400	0.32	0.46	0.22	0.31	0.46	0.23	0.05	0.93	0.02	1	1
98KD12	400	0.22	0.56	0.22	0.21	0.56	0.23	0.01	0.99	0.00	2.75	1.25
98KD9	400	0.28	0.46	0.25	0.26	0.46	0.28	0.10	0.86	0.04	4.5	1.25
98KD15	400	0.20	0.51	0.29	0.20	0.51	0.29	0.01	0.98	0.01	1.25	1
98KD17	400	0.27	0.42	0.31	0.27	0.42	0.31	0.01	0.92	0.07	2.25	1.75
98KD13	400	0.22	0.42	0.36	0.21	0.42	0.37	0.03	0.87	0.10	2	1.5
98KD14	400	0.21	0.42	0.37	0.21	0.42	0.38	0.02	0.94	0.04	1.5	0.75
11-WS-06	400	0.19	0.42	0.39	0.18	0.42	0.40	0.02	0.92	0.06	0	0.5
11-WS-07	400	0.23	0.36	0.41	0.22	0.36	0.42	0.03	0.94	0.03	2.5	1
98KD10	400	0.22	0.29	0.49	0.20	0.29	0.51	0.04	0.89	0.07	1	2.5
11-WS-11	400	0.12	0.39	0.49	0.11	0.39	0.50	0.02	0.97	0.02	0.25	0.5
98KD16	400	0.10	0.34	0.57	0.09	0.34	0.57	0.01	0.97	0.02	0.5	1.5
12-WS-04	500	0.41	0.59	0.00	0.41	0.59	0.00	0.00	0.00	0.00	0	9.4
Harts Pass Formation												
98KD18	500	0.25	0.74	0.02	0.25	0.74	0.02	0.00	0.75	0.25	1	6.4
98KD19	500	0.36	0.62	0.02	0.36	0.62	0.02	0.00	0.22	0.78	0	7
98KD21	500	0.38	0.60	0.02	0.37	0.60	0.03	0.43	0.43	0.14	0	7.4
98KD25	500	0.31	0.68	0.01	0.31	0.68	0.01	0.25	0.75	0.00	0	8.2
98KD4	500	0.31	0.67	0.03	0.29	0.67	0.04	0.32	0.53	0.16	0	8
11-HP-05	500	0.25	0.73	0.02	0.25	0.73	0.02	0.00	0.38	0.63	0	7.8
11-HP-08	500	0.36	0.63	0.01	0.35	0.63	0.02	0.56	0.44	0.00	0.6	10.8
11-HP-14	500	0.31	0.69	0.00	0.31	0.69	0.00	1.00	0.00	0.00	0	10.4
12-JMG-B-06	500	0.36	0.64	0.00	0.36	0.64	0.00	1.00	0.00	0.00	0	4.8
12-JMG-B-07	500	0.37	0.63	0.00	0.36	0.63	0.01	1.00	0.00	0.00	0	5.2
12-JMG-B-08	500	0.35	0.65	0.00	0.31	0.65	0.04	1.00	0.00	0.00	0	5.4
12-JMG-B-09	500	0.37	0.63	0.00	0.36	0.63	0.00	1.00	0.00	0.00	0	8.2
12-JMG-B-10	500	0.40	0.60	0.00	0.40	0.60	0.00	0.50	0.00	0.50	0	4
12-JMG-B-13	500	0.38	0.60	0.02	0.36	0.60	0.04	0.53	0.06	0.41	0	3.4

Note: Q, total quartz; F, total feldspar; L, lithic grains, excluding polycrystalline quartz; Qm, monocrystalline quartz; Lt, total lithic grains; Qp, polycrystalline quartz; Lv, volcanic lithic grains; Lsm, sedimentary and metamorphic lithic grains.

Fig. 3. Ternary diagrams illustrating sandstone detrital modes. Tectonic provenance fields from Dickinson et al. (1983). Q, total quartz; Qm, monocrystalline quartz; F, total feldspar; L, lithic grains, excluding polycrystalline quartz; Lt, total lithic grains.

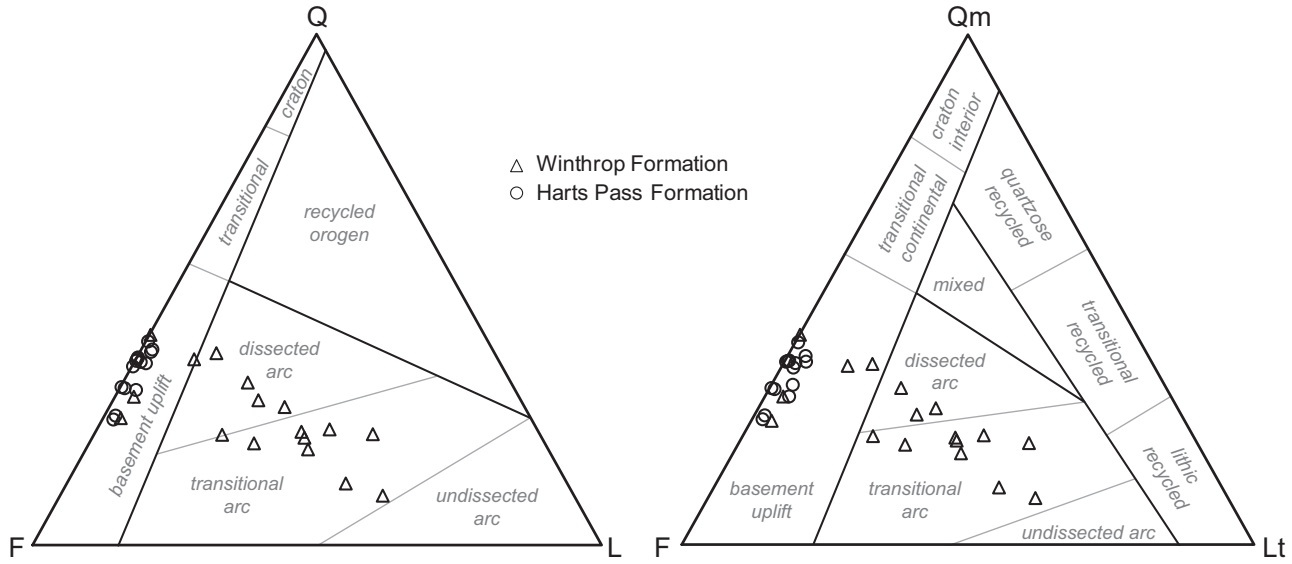

analyzed for major- and trace-element concentrations by X-ray fluorescence (XRF) and inductively coupled plasma – mass spectrometry (ICP–MS), following the procedures of Knaack et al. (1994) and Johnson et al. (1999).

Major-element geochemical results

Major elements are susceptible to mobility due to chemical weathering and diagenesis, resulting in significant geochemical changes (e.g., Nesbitt and Young 1982). The degree of weathering

can be estimated using the chemical index of alteration (CIA; Nesbitt and Young 1982). The CIA is a ratio of the mole proportions of Al_2O_3 over the sum of Al_2O_3, K_2O, Na_2O, and CaO*, where CaO* is calculated by correcting for apatite using values of P_2O_5, following the method of McLennan et al. (1993). The ratio is multiplied by 100, such that fresh igneous and metamorphic rocks have CIA values of about 50, shale rocks have CIA values of 70–75, and pure aluminosilicate weathering products, such as kaolinite, have a CIA value of 100 (Taylor and McLennan 1985; McLennan et al. 1993). CIA values for all Methow mudrock samples average 71 ± 4, typical of shales, and range from 63 to 84 (Table 3).

The index of compositional variability (ICV) is the ratio of the mole proportions of the sum of CaO, K_2O, Na_2O, Fe_2O_3, MgO, MnO, and TiO_2 over Al_2O_3, and provides a measure of the variability of the source rock types (Cox et al. 1995; Potter et al. 2005). Because minerals most susceptible to weathering tend to have high ICV values, the ICV can be applied to mudrocks as a measure of their chemical maturity (Cox et al. 1995). Chemically immature mudrocks have high ICV values and typically contain abundant silicate nonclay minerals and (or) abundant montmorillinite or sericite clays, and chemically mature mudrocks with low ICV values typically lack nonclay silicate minerals (Cox et al. 1995). ICV values for all Methow mudrock samples average 0.96 ± 0.12, and fall within a narrow range from 0.70 to 1.33 (Table 3). A plot of CIA versus ICV can help illustrate the variability of source rock type and the extent of weathering (Fig. 4A; Cox et al. 1995; Potter et al. 2005; LaMaskin et al. 2008). Almost all Methow mudrock samples plot along or between the weathering trends of andesite and basalt (Fig. 4A), suggesting similar weathering extent and low compositional variability throughout the east-derived Methow mudrocks.

Trace-element geochemical results

Trace elements (large-ion lithophile elements (LILEs), high-field-strength elements (HFSEs), and rare-earth elements (REEs)) generally have low post-depositional mobility and are strongly excluded from seawater, making them extremely useful provenance indicators (McLennan et al. 1993). La and Th are both incompatible elements that tend to be enriched in continental sources, and Sc is a compatible element enriched in mafic sources. Thus La/Sc and Th/Sc ratios both increase with increasing crustal differentiation, and are good discriminators of juvenile and evolved crust (McLennan et al. 1990, 2003). Methow samples fall within the magmatic arc field on a La–Th–Sc ternary diagram, with most samples plotting relatively close to arc andesite values along a mixing line between a more juvenile, MORB-like composition (Sc-enriched) and a more evolved source component (La- and Th-enriched; Fig. 4B). The Winthrop Formation displays more variability, with three Winthrop samples plotting with several Harts Pass Formation samples between island-arc andesite and normal mid-ocean ridge basalt (N-MORB) compositions, and two Winthrop samples plotting closer to the North American shale composite (NASC) and upper continental crust (UCC) than any other Methow samples (Fig. 4B).

A high correlation coefficient between Cr and Ni results, ultimately, from their derivation from ultramafic rocks (Garver and Royce 1993). Where Cr and Ni concentrations are anomalously high, a Cr/Ni ratio between 1.2 and 1.6 suggests an ultramafic source (Garver and Royce 1993; Garver et al. 1994). Ni and Cr abundances remain <80 ppm for all but three Methow samples; the three samples with slightly elevated Ni and Cr concentrations (up to 142 ppm Cr and 78 ppm Ni) come from both formations and are not elevated enough to require ultramafic derivation (Table 3). In fact, all Methow samples plot near the V pole on a V–Ni–(Th × 10) ternary diagram, indicating mafic source composition with little ultramafic input (Fig. 4C).

Th/Ta fractionation during subduction zone processes permits distinction between oceanic and continental sources (LaMaskin et al. 2008, after Pearce 1983). A plot of Th/Yb versus Ta/Yb can be used to assess the extent of Th/Ta fractionation, with samples plotting above the MORB array as a result of subduction enrichment of clastic sources (LaMaskin et al. 2008). Methow samples plot within the continental and fringing arc field, with Winthrop Formation samples showing greater variability than Harts Pass samples (Fig. 4D).

Chondrite-normalized rare-earth element (REE) patterns for the Methow samples indicate moderate light rare-earth element (LREE) enrichment and variable, slightly negative Eu anomalies (Fig. 4E). Eu/Eu* values range from 0.71 to 0.99 for the Winthrop Formation, with five of the seven samples showing negligible Eu anomalies (Eu/Eu* values between 0.94 and 0.99; Table 3). Eu/Eu* values range from 0.74 to 1.0 for the Harts Pass Formation, with most Harts Pass samples showing negative Eu anomalies (Eu/Eu* values between 0.80 and 0.95; Table 3). La_N/Yb_N represents the La/Yb ratio normalized to chondrite values of Taylor and McLennan (1985), and is a proxy for LREE enrichment, with high ratios of La_N/Yb_N typical of continental crustal input (Plank and Langmuir 1998; Bracciali et al. 2007; LaMaskin et al. 2008). La_N/Yb_N values range from 3.56 to 7.95 for the Winthrop Formation and from 2.92 to 6.51 for the Harts Pass Formation, with most samples showing moderate enrichment (Table 3).

Detrital zircon U–Pb analysis: methods and results

Detrital zircon was separated following standard separation procedures (e.g., DeGraaff-Surpless et al. 2002), and grains were analyzed using the Nu Plasma high-resolution (HR) multicollector (MC)–ICP–MS instrument at the Arizona LaserChron Center at the University of Arizona. Ages for grains younger than 1000 Ma are based on their $^{206}Pb/^{238}U$, while the grains older than 1000 Ma are based on $^{207}Pb/^{206}Pb$ (Gehrels et al. 2006, 2008). Data were filtered using the methods of DeGraaff-Surpless et al. (2003). $^{206}Pb/^{238}U$ ages with >10% uncertainty (1σ) are not considered further (Gehrels et al. 2006, 2008). These filtered data were plotted using Isoplot 3 (Ludwig 2008).

We determined U–Pb ages for 31 new detrital zircon samples from the Harts Pass Formation (19 samples), Winthrop Formation (10 samples), and Goat Wall unit (two samples). Samples were collected from Manning Provincial Park in southern British Columbia (northern section; 11 samples) and the Pasayten Wilderness Area and nearby regions in northern Washington State (southern section; 20 samples; Table 1). Of the 2807 grains analyzed from the Methow basin, 2780 (99%) are Mesozoic, 10 are Paleozoic (0.4%), and 17 are Precambrian (0.6%; Table S1[2]). The Mesozoic grains are largely Jurassic (1517 grains; 54% of all grains) and Early Cretaceous (1205 grains; 43%), with only 58 (2%) Triassic grains. Probability density curves for individual samples are arranged stratigraphically within the northern and southern sections, with the oldest sample at the bottom (Fig. 5). Although both the Harts Pass and Winthrop formations include Jurassic and Early Cretaceous detrital zircon age peaks through time in the basin, the relative abundance of these ages within these two formations varies considerably within the basin. Most notably, the northern section received largely Cretaceous grains (76%) and only 19% Jurassic grains, and the southern section received largely Jurassic grains (76%), with only 22% Cretaceous grains (Fig. 5). The two Goat Wall unit samples collected in the southern section record a Mesozoic age distribution similar to the underlying east-derived strata as a whole, with 59% Jurassic, 39% Cretaceous, and 2% Triassic grains (Fig. 5).

Because the samples from the Harts Pass and Winthrop formations within the northern and the southern sections have similar

[2]Supplementary data are available with the article through the journal Web site at http://nrcresearchpress.com/doi/suppl/10.1139/cjes-2013-0144.

Table 3. Methow basin mudrock geochemical data.

	XRF data: normalized major elements (wt.%)														XRF data: unnormalized trace elements (ppm)		
Sample No.	SiO_2	TiO_2	Al_2O_3	FeO*	MnO	MgO	CaO	Na_2O	K_2O	P_2O_5	Total	LOI (%)	CIA	ICV	Ni	Cr	V
11-WS-09	61.78	0.635	19.15	5.01	0.099	2.79	4.45	3.48	2.42	0.191	100	5.12	65	0.99	42	74	108
11-WS-10	56.97	0.743	18.40	11.18	0.171	5.04	2.84	2.81	1.75	0.097	100	7.75	72	1.33	85	111	153
11-WS-12	61.32	0.612	18.49	4.62	0.112	3.78	5.82	3.77	1.28	0.198	100	3.56	63	1.08	36	71	109
11-WS-16	60.72	0.741	21.38	5.30	0.094	2.14	3.33	2.67	3.60	0.018	100	5.21	69	0.84	18	30	126
11-WS-17	57.04	0.836	21.95	8.47	0.126	3.11	2.91	2.23	3.23	0.098	100	8.00	73	0.95	25	45	169
11-WS-18	57.92	0.784	20.83	8.37	0.125	2.93	3.41	2.65	2.83	0.147	100	7.10	70	1.01	26	50	160
11-WS-19	63.25	0.670	18.93	6.36	0.101	2.23	2.61	3.28	2.44	0.145	100	4.76	70	0.93	17	37	121
12JMG-B-11	62.14	0.776	19.58	6.11	0.102	3.00	2.17	3.20	2.57	0.330	100	4.83	72	0.92	28	65	169
12JMG-B-12	61.02	0.893	18.65	7.41	0.138	3.51	1.98	3.63	2.34	0.413	100	4.51	71	1.07	20	33	163
12JMG-04	60.53	0.866	19.63	6.53	0.122	2.89	2.86	3.36	3.03	0.188	100	1.41	68	1.00	25	49	198
12JMG-07	60.26	0.889	19.67	7.16	0.124	3.68	2.47	2.98	2.59	0.189	100	3.24	71	1.01	57	91	196
12JMG-10	58.47	1.009	21.80	6.26	0.089	2.87	2.47	3.30	3.58	0.131	100	5.21	70	0.90	21	66	164
12JMG-12	62.65	0.821	18.72	6.70	0.135	3.12	1.82	4.18	1.66	0.194	100	3.99	71	0.98	21	39	173
12JMG-13	63.07	0.712	17.55	6.77	0.131	3.07	3.33	4.01	1.19	0.174	100	3.71	68	1.09	22	40	152
12JMG-14	63.08	0.784	18.00	7.27	0.126	3.09	2.28	3.62	1.55	0.184	100	4.25	71	1.04	22	44	166
12JMG-15	62.17	0.893	20.02	6.54	0.100	3.06	1.16	3.61	2.27	0.172	100	4.45	74	0.88	24	52	181
12JMG-16	60.55	0.944	19.85	6.94	0.110	3.17	2.73	3.21	2.28	0.198	100	4.61	71	0.98	23	53	198
12JMG-18	62.09	0.788	18.34	6.75	0.128	3.19	2.82	4.07	1.62	0.188	100	3.91	69	1.06	23	43	166
11-HP-10	65.74	1.075	18.15	8.44	0.090	2.81	0.46	1.62	1.49	0.132	100	4.96	84	0.88	78	142	199
11-HP-11	60.09	0.831	23.38	6.18	0.100	2.77	0.55	1.35	4.63	0.110	100	6.01	78	0.70	20	37	140
11-HP-13	60.74	0.883	20.08	6.20	0.107	2.86	2.74	3.31	2.85	0.235	100	3.70	70	0.94	35	59	174
11-HP-02	59.14	0.785	21.28	6.22	0.124	2.69	2.81	3.09	3.67	0.212	100	4.84	69	0.91	19	28	122
11-HP-04	59.15	0.921	23.09	6.69	0.086	2.66	1.12	2.44	3.59	0.255	100	6.87	77	0.76	24	46	177
11-HP-06	60.80	0.878	20.18	6.43	0.146	3.14	2.84	3.59	1.68	0.323	100	4.51	72	0.93	24	46	149
11-HP-15	62.93	0.777	19.64	5.81	0.104	2.57	1.82	3.39	2.68	0.272	100	3.68	72	0.87	25	55	174

	ICP–MS data: unnormalized trace elements (ppm)																												
Sample No.	La	Ce	Pr	Nd	Sm	Eu	Gd	Tb	Dy	Ho	Er	Tm	Yb	Lu	Ba	Th	Nb	Y	Hf	Ta	U	Pb	Rb	Cs	Sr	Sc	Zr	Eu/Eu*	La_N/Yb_N
11-WS-09	16.20	33.03	4.22	16.79	3.57	1.05	3.03	0.46	2.74	0.54	1.48	0.21	1.38	0.22	1231	4.07	6.59	14.23	2.89	0.44	2.61	10.35	53.6	1.03	755	12.1	102	3.26	7.95
11-WS-10	28.07	54.57	7.07	28.02	5.92	1.43	5.27	0.82	4.90	0.95	2.66	0.39	2.48	0.39	701	5.90	9.18	25.59	4.46	0.63	2.54	8.64	47.4	2.98	425	14.6	166	4.00	7.64
11-WS-12	11.74	24.88	3.22	13.20	2.94	0.88	2.52	0.38	2.28	0.47	1.23	0.19	1.15	0.19	860	3.23	5.92	11.72	2.59	0.40	1.71	8.93	23.0	0.59	870	11.5	97	3.00	6.9
11-WS-16	17.72	36.88	4.71	19.23	4.55	0.97	3.89	0.65	4.07	0.79	2.21	0.33	2.17	0.35	1042	5.16	8.86	21.07	4.80	1.06	2.56	11.07	108.0	7.52	401	17.3	177	3.23	5.53
11-WS-17	12.32	22.92	3.45	14.80	3.75	1.21	3.97	0.68	4.28	0.88	2.44	0.37	2.33	0.38	677	1.97	3.15	23.38	2.79	0.20	1.76	8.62	101.0	6.37	276	24.5	93	7.89	3.57
11-WS-18	11.93	24.60	3.40	14.60	3.73	1.17	3.87	0.63	3.94	0.81	2.26	0.34	2.15	0.35	837	2.31	4.51	21.94	2.72	0.29	1.87	8.50	81.4	5.87	364	20.7	93	6.26	3.74
11-WS-19	11.27	18.90	3.08	13.15	3.20	1.03	3.25	0.53	3.32	0.69	1.92	0.29	1.87	0.31	815	2.48	4.74	18.71	3.04	0.32	1.86	10.08	63.9	2.88	369	17.3	102	4.93	4.08
12JMG-B-11	10.53	12.96	2.51	10.59	2.42	0.74	2.36	0.38	2.34	0.48	1.35	0.21	1.47	0.25	970	3.53	6.64	13.41	3.12	0.44	2.15	10.16	72.4	4.09	485	17.9	106	2.95	4.84
12JMG-B-12	16.89	35.08	4.60	19.03	4.44	1.13	4.25	0.69	4.23	0.84	2.34	0.34	2.22	0.35	517	3.98	8.81	22.94	2.90	0.57	1.98	10.10	65.8	3.49	353	15.9	96	4.54	5.15
12JMG-04	11.51	25.28	3.55	15.63	4.03	1.22	4.24	0.73	4.55	0.97	2.72	0.41	2.67	0.43	995	2.46	4.34	24.73	2.90	0.30	1.35	8.50	65.3	2.86	467	24.3	99	6.97	2.92
12JMG-07	14.32	29.73	4.13	17.56	4.37	1.41	4.51	0.75	4.73	0.97	2.72	0.41	2.62	0.42	731	3.24	5.14	24.96	3.09	0.35	1.76	10.40	64.9	4.24	415	23.6	109	6.26	3.69
12JMG-10	16.96	35.31	4.61	19.33	4.53	1.26	4.31	0.70	4.41	0.93	2.63	0.40	2.64	0.43	1290	4.29	6.85	24.55	3.60	0.46	2.06	11.45	82.9	2.88	397	23.7	125	4.95	4.33
12JMG-12	10.86	24.27	3.24	14.01	3.51	1.12	3.63	0.63	3.94	0.82	2.32	0.34	2.19	0.36	444	2.50	3.58	20.69	2.91	0.25	1.23	7.20	38.6	1.87	459	22.0	100	6.42	3.36
12JMG-13	11.10	23.35	3.14	13.47	3.33	0.99	3.34	0.55	3.47	0.71	1.98	0.29	1.88	0.30	421	2.39	3.67	18.41	2.68	0.26	1.18	9.03	27.5	1.61	300	18.9	92	5.88	3.99
12JMG-14	11.89	23.37	3.45	15.23	3.96	1.28	4.19	0.71	4.37	0.92	2.47	0.36	2.21	0.35	505	2.10	3.26	24.25	2.62	0.22	1.01	9.62	34.2	2.46	384	21.0	89	8.30	3.63
12JMG-15	12.14	27.24	3.42	14.39	3.39	0.97	3.10	0.54	3.34	0.70	2.04	0.32	2.09	0.34	612	2.75	4.07	16.82	3.13	0.28	1.30	6.92	48.6	3.66	363	23.3	107	4.72	3.92
12JMG-16	12.41	26.67	3.70	16.43	4.24	1.29	4.36	0.74	4.66	0.96	2.69	0.41	2.55	0.41	701	2.66	3.90	24.21	3.04	0.26	1.29	5.96	48.3	3.01	330	26.1	103	7.03	3.28
12JMG-18	11.35	24.04	3.25	13.95	3.45	1.07	3.54	0.60	3.75	0.77	2.13	0.32	1.99	0.33	509	2.51	3.65	19.25	2.61	0.25	1.27	7.44	37.1	2.20	354	20.2	88	6.24	3.85
11-HP-10	13.27	29.02	3.91	16.65	4.15	1.15	4.38	0.77	4.84	1.03	2.92	0.42	2.70	0.43	565	2.85	6.84	25.15	3.32	0.46	1.46	7.49	41.7	4.14	149	26.7	119	5.28	3.32
11-HP-11	13.77	27.59	3.77	16.15	4.01	0.97	4.02	0.63	3.80	0.76	2.10	0.32	2.00	0.33	1461	2.86	5.76	20.23	2.39	0.38	2.19	6.38	93.8	10.15	120	18.8	77	5.45	4.65
11-HP-13	17.44	37.65	4.85	20.36	4.87	1.41	4.91	0.80	4.90	1.00	2.79	0.41	2.65	0.45	920	3.75	7.06	26.66	4.35	0.49	2.21	7.27	78.1	8.61	415	20.5	147	4.81	4.45
11-HP-02	14.07	27.99	3.92	16.06	3.70	1.08	3.55	0.57	3.39	0.69	1.94	0.29	1.85	0.30	1237	3.00	8.15	19.40	2.59	0.52	2.20	11.21	100.8	5.94	482	14.2	85	4.22	5.14
11-HP-04	18.77	32.59	4.69	19.04	4.18	1.29	3.76	0.60	3.52	0.74	2.02	0.30	1.95	0.33	1056	3.63	7.60	20.33	3.30	0.47	2.15	14.07	90.6	2.89	263	18.6	116	4.06	6.51
11-HP-06	18.31	37.91	4.87	19.91	4.61	1.29	4.55	0.78	4.83	1.01	2.83	0.44	2.86	0.47	748	5.04	9.60	25.05	3.64	0.85	3.21	9.03	38.4	1.47	359	20.5	122	4.24	4.33
11-HP-15	14.29	32.56	3.97	16.74	4.14	1.15	4.12	0.70	4.36	0.88	2.49	0.38	2.48	0.42	828	3.52	6.93	23.55	3.33	0.46	2.04	8.96	72.3	6.35	388	18.9	113	4.90	3.89

Note: FeO* is total iron reported as FeO. LOI, loss on ignition. $Eu/Eu^* = Eu_N/(Sm_N + Gd_N)^{0.5}$ where N is concentration in ppm normalized by chondrite values of Taylor and McLennan (1985).

Fig. 4. (A) Plot of the chemical index of alteration (CIA) versus index of chemical variability (ICV), after Potter et al. (2005). ICV values for andesite from Ewart (1982), and for basalt and granite from Li (2000). (B) Ternary plot of La–Th–Sc, after McLennan et al. (1990). The magmatic arc-related and passive continental margin fields (after Girty et al. 1993) are derived from samples listed in McLennan et al. (1990). N-MORB, normal mid-ocean ridge basalt; NASC, North American shale composite; UCC, upper continental crust; values from Taylor and McLennan (1985) and McLennan et al. (2003). (C) Ternary plot of V–Ni–(Th × 10) after Bracciali et al. (2007). (D) Th/Yb versus Ta/Yb diagram after Pearce (1983). Th/Ta fractionation occurs during subduction zone processes; the degree of subduction enrichment of clastic sources increases with positive slope (LaMaskin et al. 2008). Source region values are from Taylor and McLennan (1985) and McLennan et al. (2003). (E) Chondrite-normalized REE diagram for all Methow mudrocks (normalization values of Taylor and McLennan 1985).

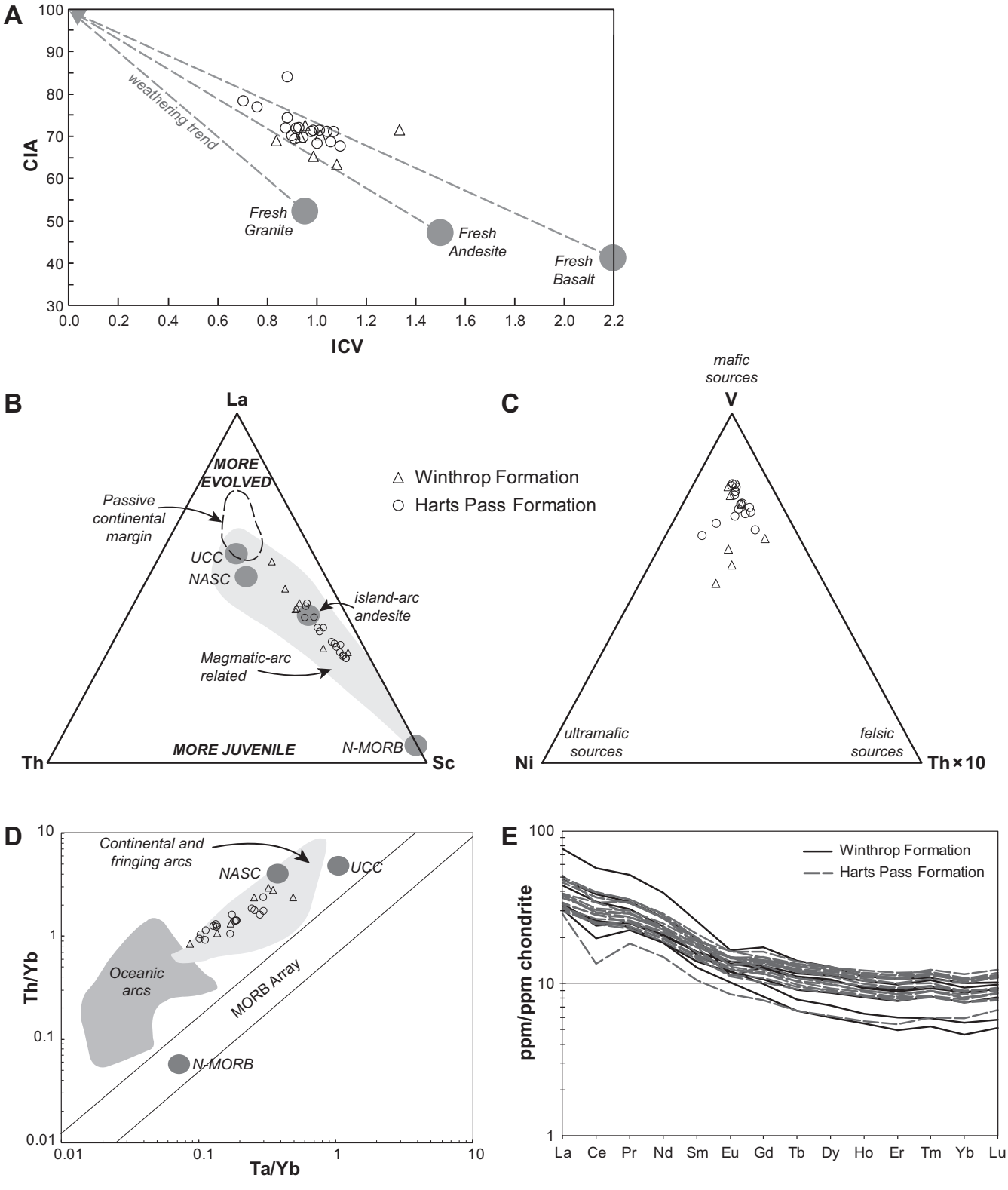

Fig. 5. Histograms and superimposed probability density plots of detrital zircon age data for Mesozoic grains in the Harts Pass Formation, Winthrop Formation, and Goat Wall unit from northern (E.C. Manning Provincial Park) and southern (Pasayten Wilderness and adjacent regions) portions of the Methow basin. Samples are arranged in stratigraphic order, with the oldest at the bottom. Depositional age range is indicated by light grey bar. *n*, number of samples.

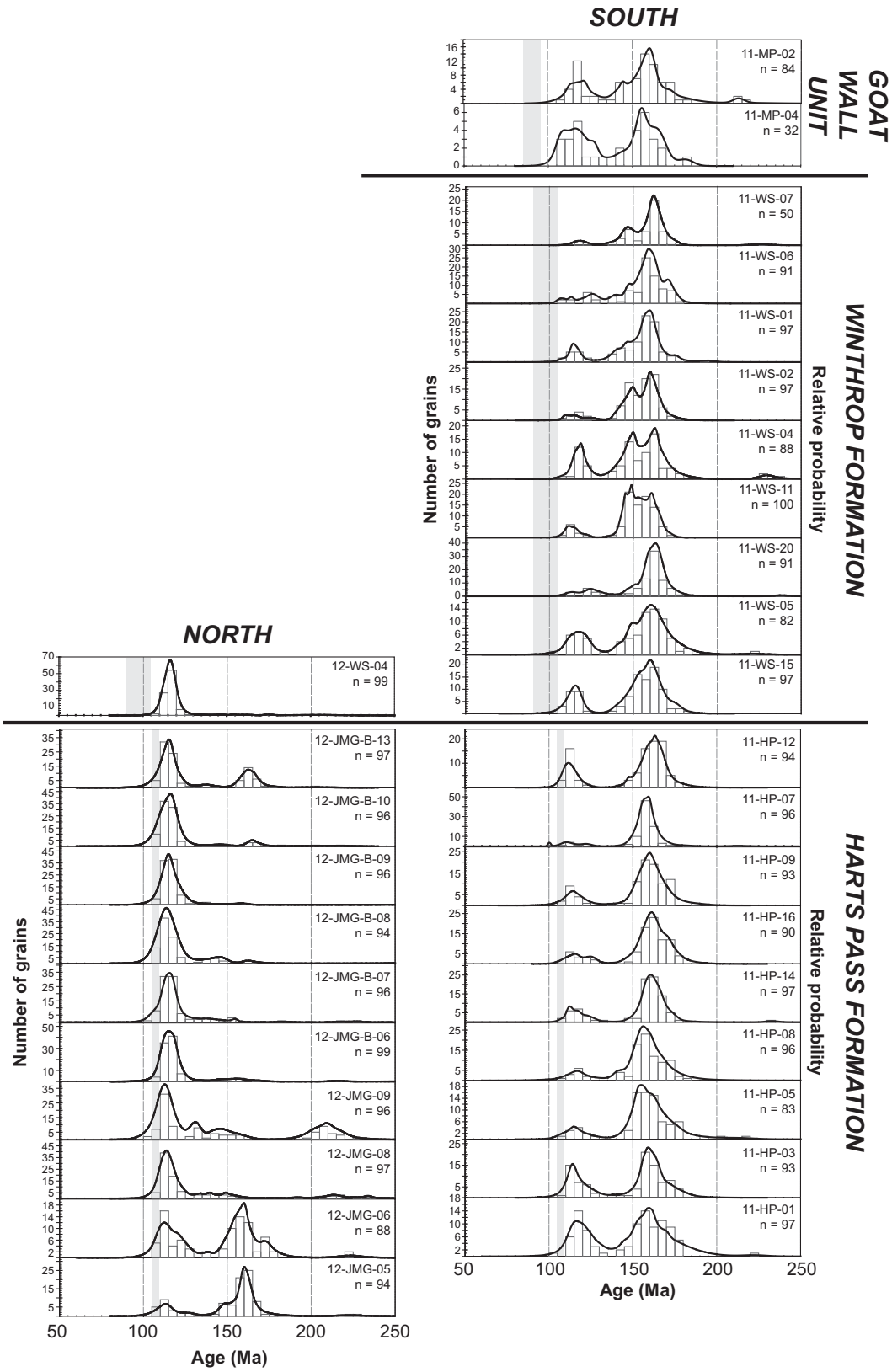

Fig. 6. Composite histograms and superimposed probability density plots of detrital zircon age data for Mesozoic Harts Pass and Winthrop Formation grains in the northern and southern portions of the Methow basin.

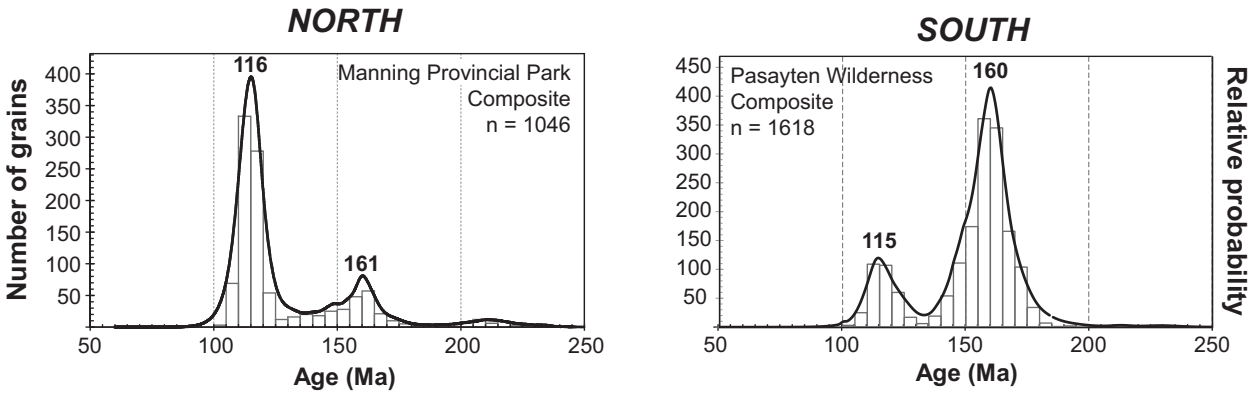

Mesozoic age peaks, we plot all grains from each section together (excluding the overlying Goat Wall unit samples) to generate composite probability density curves that characterize the age populations of the northern and southern samples (Fig. 6). In both the northern and southern sections of the Harts Pass and Winthrop formations, Cretaceous grains form one peak at 115–116 Ma, including a range of ages from 100 to 125 Ma, and a Jurassic peak at 161 Ma that includes 140–180 Ma grains (Fig. 6). Moreover, both sections include relatively few grains between 125–140 Ma (85 grains; 3% of all grains) and 200–252 Ma (55 grains; 2% of all grains). Combining all 27 pre-Mesozoic grains from all samples into one probability density curve reveals small peaks at 278, 512, 540, 700, 1035, and 1190 Ma (Fig. 7).

Fig. 7. Composite histogram and superimposed probability density plot of pre-Mesozoic grains from the Harts Pass and Winthrop formations.

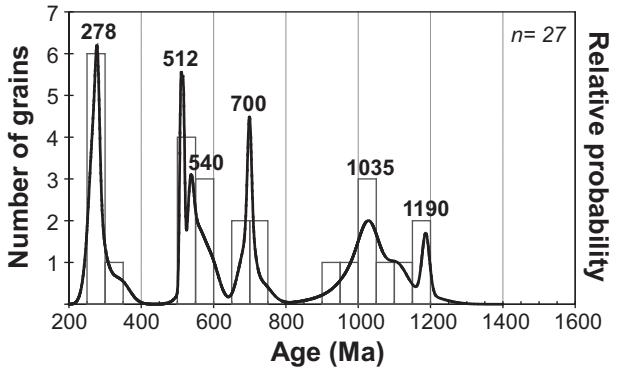

Detrital zircon Hf analysis: methods and results

Hafnium isotope ratios from detrital zircon grains provide another source fingerprint. In addition to the radioactive decay of ^{176}Lu to stable ^{176}Hf, fractionation during partial melting of the mantle leads to Hf-enriched partial melt and residual mantle depleted in Hf and enriched in Lu (Amelin et al. 1999; Kinny and Maas 2003). Because zircon crystals easily incorporate Hf but not Lu, without additional ^{176}Lu to decay to ^{176}Hf, the ratio of ^{176}Hf to the stable isotope ^{177}Hf in the zircon essentially stays constant after formation of the zircon crystal. In contrast, the enrichment of ^{176}Lu in the residual mantle due to fractionation during partial melting means that the mantle's ^{176}Hf/^{177}Hf ratio increases with time as more ^{176}Lu decays to ^{176}Hf (e.g., Kinny and Maas 2003). The geochemical signature of the zircon crystal is described in terms of epsilon (ε) units, where more positive ε_{Hf} values indicate juvenile sources extracted from the mantle more recently and therefore record higher ^{176}Hf/^{177}Hf, and negative ε_{Hf} values indicate evolved sources that were originally extracted from the mantle prior to significant fractionation, and therefore record lower ^{176}Hf/^{177}Hf.

Hf isotopic data were measured by the Nu Plasma HR MC–ICP–MS instrument at the Arizona LaserChron Center at the University of Arizona using a 40 μm spot placed over the same area ablated for U–Pb age data for selected Jurassic and Early Cretaceous zircon grains from the Harts Pass and Winthrop Formation samples. All of the zircon grains exhibit positive ε_{Hf} values within the range of +1.1 to +15.1 (Fig. 8; Table S2[2]). The Early Cretaceous grains (105–121 Ma) have a mean ε_{Hf} value of +10.0 ± 1.5 (number of samples (n) = 366). Two outliers in this Cretaceous age range have an ε_{Hf} value of +3.3 and +4.7, but most of the grains in this population are tightly grouped between +7 to +13 (Fig. 8). The Late Jurassic to Early Cretaceous grains (130–150 Ma) have a mean ε_{Hf} value of +9.0 ± 2.8 (n = 97), and include the widest range of ε_{Hf} values, from +1.1 to +15.1 (Fig. 8). The Middle to Late Jurassic grains (152–174 Ma)

Fig. 8. Detrital zircon ε_{Hf} versus age plot for selected zircon grains from both the Harts Pass and Winthrop formations. The ranges of zircon ε_{Hf} values measured in Jurassic through Eocene plutons intruded into the Coast Shear Zone and Intermontane superterrane (eastern Coast Mountains batholith (CMB); values from Cecil et al. 2011) as well as the depleted mantle (DM) array ε_{Hf} (500–0 Ma) (values from Vervoort and Bichert-Toft 1999) are shown to the right of the Methow data for comparison.

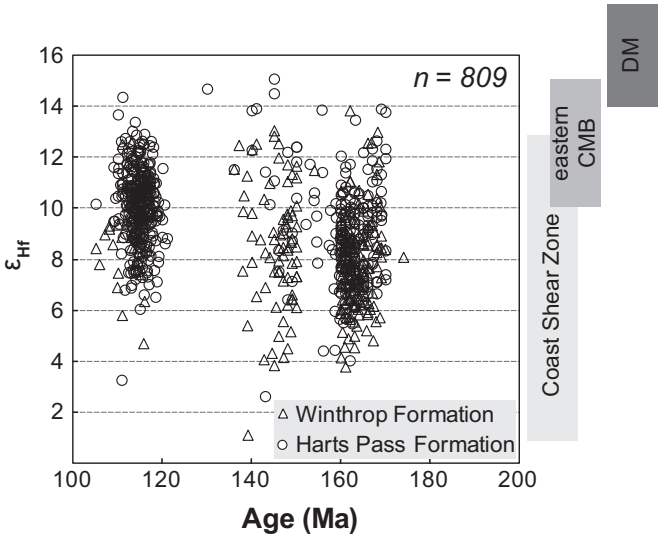

have a mean ε_{Hf} value of +8.4 ± 1.9 (n = 346), and range from +3.8 to +13.9, with most grains between +5 and +11 (Fig. 8).

Discussion

Depositional age and sedimentation rates of the east-derived Methow basin strata

Ammonite fragments collected from the upper Harts Pass Formation near Harts Pass were originally identified as Albian, but additional species discovered at the same locality were identified as Aptian to Albian, and the upper Harts Pass Formation was considered upper Aptian by Barksdale (1975). However, middle Albian ammonite fauna from other localities within the Harts Pass Formation and Albian fossils from shallow-water deposits at Dead Lake, stratigraphically below the Harts Pass Formation, led Haugerud et al. (1996) to consider the Harts Pass Formation middle Albian. An Albian depositional age is consistent with our youngest detrital zircon ages in the basal Harts Pass Formation samples in the southern section (11-HP-01 and 11-HP-03) that yield weighted mean ages of 112 ± 4 and 112 ± 2 Ma, respectively. Likewise, the youngest clusters of five grains in the lowest two Harts Pass-correlative samples collected from the northern section (12-JMG-05 and 12-JMG-06) yield weighted mean ages of 109 ± 4 and 108 ± 3 Ma, respectively. These detrital zircon results are also consistent with young detrital zircon fission track peak ages that limit the maximum depositional age of the Harts Pass-correlative upper Jackass Mountain Group strata in Manning Park to late Albian (105–97 Ma; Garver and Brandon 1994). Taken together, these results suggest a middle (109–105.3 Ma; Albian substages from Fiet et al. 2001) to late Albian age (105.3–99.6 Ma; Fiet et al. 2001) of deposition for the Harts Pass Formation.

Haugerud et al. (1996) considered the Winthrop Formation Cenomanian to Turonian(?) based on its interfingering relationship with the Cenomanian–Turonian(?) Virginian Ridge Formation, a 97.5 +2/–3 Ma sill that intrudes the Winthrop Formation, and crosscutting 88–90 Ma stocks. However, Miller et al. (2006) assigned a middle to late Albian age to the Winthrop Formation, based on a megafloral assemblage characterized by species that require an age no younger than late Albian. The youngest three detrital zircon grains within each of the two basal Winthrop Formation samples yield weighted mean ages of 107.2 ± 7.4 Ma (11-WS-15 in the southern Methow) and 109.8 ± 4.3 Ma (12-WS-04 in Manning Park), consistent with middle Albian or younger deposition. Enkin et al. (2002) reported detrital zircon as young as 94.3 ± 4.2 Ma from the upper Winthrop Formation, suggesting Turonian or younger deposition. Together, these biostratigraphic and U–Pb age results suggest late Albian through Turonian deposition of the Winthrop Formation.

These depositional age constraints for Harts Pass Formation permit up to 10 million years (109–99.6 Ma) for deposition, and only 4 million years if Harts Pass deposition was limited to the middle Albian only (109–105.3 Ma). Deposition of up to 3200 m of the Harts Pass Formation within these time constraints requires rapid sedimentation rates ranging from 0.3 mm/year to as high as 0.8 mm/year. Winthrop Formation sedimentation rates may have averaged as high as 0.26 mm/year (up to 4000 m deposited over 15 million years), but more specific estimates of sedimentation rates are difficult to determine, given the variability in the thickness of the Winthrop Formation (300–4000 m).

Characterizing the source of the east-derived Methow basin strata

Consistently west-directed paleocurrent indicators suggest that the Methow source region was located east of the basin; the source area could have extended northeast and (or) southeast of the basin, with sediment then transported into the basin from the east.

Petrographic analysis of the Harts Pass and Winthrop Formation sandstone reveals poor sorting, low matrix content, and angular clasts, suggesting proximal, first-cycle sediment. The Harts Pass Formation contains very few volcanic lithic grains and abundant monocrystalline quartz and feldspar, suggesting a plutonic source. The Winthrop Formation has more variable volcanic lithic content, which ranges from 0% to 57% of the sample, with the lowest lithic content at the base of the Winthrop Formation. This increase in volcanic lithic grains suggests an Early Cretaceous pulse of volcanic activity adjacent to the basin, which may presage Late Cretaceous volcanic activity within the Methow basin, as recorded by the overlying Goat Wall unit. Metamorphic and sedimentary lithic grains are rare in both the Harts Pass and Winthrop formations, comprising up to 3% of a single sample and typically less than 1%.

Because mudrocks are deposits of the most weathered and well-mixed source material, they tend to record the mafic provenance record that is not well represented in sandstone petrography or detrital zircon analysis. Mudrock geochemistry reveals that the source region for the east-derived Methow strata was geochemically juvenile, with compositions typical of island-arc andesite and basalt. REE distributions show moderate LREE enrichment and variable, slightly negative Eu anomalies, typical of young, undifferentiated magmatic arcs involving little or no involvement of continental crust (Gromet and Silver 1987; McLennan et al. 1993). The Harts Pass Formation shows less variability than the Winthrop Formation, and neither formation contains evidence of either significant ultramafic input or continental crust enrichment (Fig. 4).

The U–Pb ages of detrital zircon from the Harts Pass and Winthrop formations and the Goat Wall unit record a Mesozoic age signature dominated by Middle to Late Jurassic and Early to middle Cretaceous zircon grains. Felsic plutonic sources are most likely to provide the majority of detrital zircon grains found in these Methow samples. Zircon requires significant available silica and oxygen to form, and tends to crystallize late in the crystallization process because zirconium is incompatible in common silicate minerals. Cathodoluminescence (CL) images of the Methow zircon grains show oscillatory zoning that would be expected for a zircon from a plutonic source (Hoskin and Schaltegger 2003), and they lack inherited cores visible in CL or evident in the age data, that might be expected from metamorphic sources or more complex plutonic sources. Moreover, Methow zircon grains retain a euhedral shape and are typically larger than 100 μm, unlike smaller, thinner zircon lacking concentric zoning that are more typical of volcanic sources (Hoskin and Schaltegger 2003). Methow zircon grains apparently have not been recycled from sedimentary or metasedimentary rocks and undergone processes which would have abraded and rounded them. The Mesozoic age signature also suggests that there was not time to recycle these grains prior to deposition in the Methow basin.

The dominantly Mesozoic age signature in the detrital zircon U–Pb record of the Harts Pass and Winthrop formations and the Goat Wall unit indicates that the plutonic source for these rocks was active from about 170 to 145 Ma and again from 125 to 105 Ma, with little magmatic activity between 145 and 125 Ma (Fig. 6). Significantly, the northern Harts Pass and Winthrop samples record a dominantly Cretaceous source signature, while the southern Harts Pass and Winthrop samples record a dominantly Jurassic source signature (Fig. 6). These spatial differences may record similar spatial relationships between Jurassic and Cretaceous plutons exposed within the source area. A few Triassic grains suggest earlier Mesozoic magmatic activity, but these grains do not form a robust peak. Most Paleozoic and Precambrian zircon grains occur in only a few samples, and comprise only 1% of the total grains analyzed, suggesting that the primarily Middle to Late Jurassic and Early Cretaceous magmatic arc immediately east of the Methow basin acted as a topographic barrier to sediment transport from sources further east.

Detrital zircon ε_{Hf} values from Jurassic and Cretaceous grains throughout the Harts Pass and Winthrop formations record a juvenile geochemical signature that becomes increasingly positive with time, from an average of +8.4 for Middle to Late Jurassic grains to +10 for Early Cretaceous grains (Fig. 8). This universally juvenile geochemical signature indicates that the Jurassic and Cretaceous magmatic source of detrital zircon intruded west of the Precambrian craton and did not experience significant interaction with more evolved, continental rocks. These results are consistent with our mudrock geochemical results and with an earlier neodymium study of Methow strata that suggested a primitive sediment source (Barfod and Nelson 1992).

Taken together, the provenance data presented here describe a proximal, largely dissected, geochemically juvenile, Jurassic and Early Cretaceous magmatic arc source that formed a topographic upland east of the Methow basin from middle Albian through at least Turonian(?) time.

Provenance of east-derived Methow strata

The southern Canadian Cordillera can be broadly divided into the plutonic rocks associated with the Intermontane terranes (Stikine and Quesnel terranes), the Coast Mountains batholith, and the Okanogan Range and Omineca Crystalline belt in present-day southeastern British Columbia and Washington State (Fig. 1; Petö 1974; Armstrong 1988; Hurlow and Nelson 1993; Erdmer et al. 2001; Gehrels et al. 2009). Magmatism has been active in the region since the Proterozoic, but the largest magmatic fluxes occurred during the Middle Jurassic through the Late Cretaceous (Petö 1974; Armstrong 1988; Gehrels et al. 2009).

Gehrels et al. (2009) compiled age dates from 313 zircon and 59 titanite grains and found that magmatic activity in the Coast Mountains batholith occurred in four main belts of distinct ages: 160–140, 120–100, 100–80, and 60–48 Ma. Gehrels et al. (2009) presented a schematic model for the tectonic evolution of the southern Coast Mountains batholith, in which at least 800 km of sinistral (southward) motion following the mid-Jurassic juxtaposition of the Insular superterrane against the Stikine and Yukon–Tanana terranes (McClelland et al. 1992) means that the present-day western part of the southern Coast Mountains batholith represents the northern continuation of the present-day eastern portion of the batholith. The Gehrels et al. (2009) schematic model considers plutonic rocks intruded into the western Intermontane superterrane, including the Quesnel terrane in the southern British Columbia, to be part of the eastern belt of magmatism associated with the Coast Mountains batholith.

The Coast Mountains batholith experienced a magmatic lull from 140 to 120 Ma, followed by another magmatic flux event beginning at 120 Ma, with these younger plutons intruding immediately east of the older magmatic belt, and migrating eastward through Late Cretaceous time (Gehrels et al. 2009). Cecil et al. (2011) found that ε_{Hf} values for the Coast Mountains batholith were most strongly controlled by which terrane a given pluton intruded. Plutons intruded into the Alexander terrane (Insular superterrane; western belt) yield zircon ε_{Hf} values between +6 and +8, plutons intruded into the Stikine terrane (Intermontane superterrane; eastern belt) yielded zircon ε_{Hf} between +10 and +15, and plutons intruded into a belt of mid-Cretaceous thrust faults between the eastern and western belts yielded the widest range of ε_{Hf} values, from +1.5 to +11.6 (Cecil et al. 2011).

The Eagle Plutonic complex east of the Pasayten fault in southern British Columbia intruded the Quesnel terrane of the western Intermontane superterrane and would be considered part of the eastern belt of the Coast Mountains batholith, as broadly defined by Gehrels et al. (2009). The Eagle Plutonic complex includes Middle to Late Jurassic tonalite and gneiss (157–148 Ma) that are crosscut by the 111 Ma Fallslake Plutonic suite (Grieg et al. 1992). The Eagle Plutonic Complex was uplifted, cooled, and unroofed in mid-Cretaceous time along the Pasayten fault (Grieg et al. 1992).

In Washington state, the western Okanogan Range is bounded by the Pasayten fault to the west and includes Jurassic and Cretaceous plutons (including the Similkameen pluton; Petö 1974) that range in age from 166 to 154 Ma (Rb–Sr dates, consistent with K–Ar dates; Petö and Armstrong 1976) and from 114 to 110 Ma (U–Pb dates; Grieg et al. 1992; Hurlow 1993). Hurlow and Nelson (1993) concluded that the 114–110 Ma plutons of the Okanogan Range represent an older, southerly segment of the late Albian volcanic rocks of the Spences Bridge Group in British Columbia, and defined the Okanogan – Spences Bridge arc as a >300 km long north-northwest-trending Early Cretaceous magmatic arc intruded into the western margin of the Intermontane superterrane. This Okanogan – Spences Bridge arc would be included within the 120–100 Ma belt of magmatism within the southeastern belt of the Coast Mountains batholith described by the Gehrels et al. (2009) schematic model.

The mean $^{87}Sr/^{86}Sr$ value for the Jurassic Okanagan plutons is 0.7042, consistent with magma derivation from metabasic rocks without input of older, continental crustal material (Petö and Armstrong 1976). Zircon ε_{Hf} values from these rocks would likely reflect this juvenile geochemical signature. However, plutons east of Okanogan Lake have initial $^{87}Sr/^{86}Sr$ values of 0.705–0.707, indicating that this region straddles the edge of Precambrian basement (Petö and Armstrong 1976).

The Methow basin formed on the southern Methow block, which would have been in a forearc position relative to the Jurassic–Cretaceous magmatic arc of the southern Canadian Cordillera and northern Washington State (Monger et al. 1994; DeGraaff-Surpless et al. 2003; Gehrels et al. 2009); however, the exact position of Methow basin relative to this long, north-south-trending magmatic arc has clearly been modified by younger brittle, dextral strike-slip motion along the Pasayten fault (e.g., Grieg 1992; Hurlow 1993). Methow sediment sources must have been almost entirely limited to sources just east of the middle Cretaceous Pasayten fault, and included only a few grains from other potential sources further east, including eastern Okanogan intrusive rocks. Rocks in the Omineca Crystalline belt include hornblende- and biotite-bearing granodiorite, leucocratic quartz monzonite, and granite (Carr 1991). Zircons from these rocks are Precambrian (3300–1800 Ma) and Mesozoic (240, 190–170, and 90 Ma; Carr 1991; Ross and Parrish 1991), and this region contains basement rocks of the North American craton (Ross and Parrish 1991; Carr 1995). Therefore, detrital zircon from the Omineca Crystalline belt would include abundant Precambrian zircons with a more evolved geochemical signature (Ross and Parrish 1991; Carr 1995) as well as evidence of Paleozoic plutonism (Carr 1991), neither of which are significant in the Methow detrital zircon provenance record. Therefore, the eastern belt of the Coast Mountains batholith, including the Eagle Plutonic Complex located south of the Gehrels et al. (2009) study area, and the westernmost Okanogan Range likely acted as proximal and localized sediment sources within the southern Canadian Cordillera, and formed a topographic barrier during Albian–Turonian time that blocked almost all sediment transport from the rest of the region.

Tectonic implications of Methow provenance

Our interpretation of an eastern Coast Mountains batholith – western Okanogan Range source for the east-derived strata of the Methow basin is consistent with previous studies that document rapid Albian uplift and unroofing of plutons east of the Methow basin (Grieg 1992; Hurlow 1993; Garver and Brandon 1994; Kiessling 1998). The Pasayten fault likely served as the locus for this early Albian uplift of eastern sources; in Washington State, the Pasayten fault zone includes a 1 km thick mylonitic shear zone that records sinistral transcurrent displacement with a component of down-to-the-west slip (Hurlow 1993). Hurlow (1993) concluded that emplacement of the 111–114 Ma plutons within the western Okanogan Range batholith was controlled by dip-slip in a steeply

dipping, northwest-striking fault zone, with deformation ending by 100 Ma. Hurlow (1993) considered this early east-side-up dip-slip component to be extensional. However, sinistral oblique slip on the Pasayten fault was coeval with contraction along the Methow River thrust zone to the south, which Hurlow (1993) inferred was due to counterclockwise rotation of the southern Methow block. Alternatively, sinistral oblique motion on the Pasayten fault has been interpreted as transpressional along a steeply dipping reverse fault (Grieg 1992). Grieg et al. (1992) suggest that the ductile strain in the 110.5 ± 2 Ma Fallslake plutonic suite of the Eagle Plutonic complex in southern British Columbia developed during sinistral, east-side-up reverse displacement, with northeast-dipping foliation indicating a northeast-dipping orientation for the Pasayten fault during transpressional ductile shear.

Our preferred model for middle Cretaceous evolution of the Methow basin begins with Early Cretaceous arc magmatism east of the basin that supplied abundant volcanic lithic and plutonic material into the older basin strata in large deltaic and shallow marine deposits of the northern Methow block (e.g., the lower and middle Jackass Mountain Group; Fig. 9A; MacLaurin et al. 2011). Sinistral transpression during the late Early Cretaceous as western Cordilleran terranes of the Insular superterrane moved south (following the schematic model of Gehrels et al. 2009) was partially accommodated along the Pasayten fault. Rapid early Albian uplift along the Pasayten fault exposed Jura-Cretaceous plutonic rocks to erosion by middle Albian time, providing a proximal sediment source for the lithic-poor Harts Pass Formation and also forming a significant barrier to transport of sediment into the Methow basin from regions further east (Fig. 9B). Sinistral transpression also resulted in emergence of the Bridge River and Hozameen terranes, forming the western margin of the Methow basin recorded by westerly derived sedimentation in the Methow basin. Maximum subsidence of the Methow trough occurred during the middle Albian, as terranes both west and east of the basin were uplifted. The thick turbiditic sandstone and shale of the Harts Pass Formation were rapidly deposited in the subsiding and underfilled Methow basin from newly uplifted and unroofed plutons to the east, while less abundant chert-rich detritus of the Jackita Ridge Formation reached the Methow basin from the west (Fig. 9B).

By late Albian time, large-scale sinistral translation of the Insular superterrane and associated uplift of eastern sources along the Pasayten fault ended, and the region underwent compression as the Insular superterrane fully accreted to the western margin of North America (cf. Gehrels et al. 2009). During the late Albian, the Methow basin nearly filled with sediment, and compression along the western margin further uplifted the Bridge River terrane and produced at least local unconformity within the Methow basin (Fig. 9C). Without continued eastern uplift after middle Albian time, the proximal portion of the eastern magmatic arc was progressively dissected, permitting drainage systems to reach further east into the still partially intact volcanic carapace, leading to greater lithic volcanic input into the Winthrop Formation while maintaining a consistent Jura-Cretaceous detrital zircon age and Hf signature, and consistent mudrock geochemistry. West-derived strata of the Virginian Ridge Formation interfingered with east-derived strata of the Winthrop Formation in late Albian through Turonian fluvial and deltaic systems that formed with local unconformity on top the middle Albian Harts Pass Formation.

By Turonian time, continued compressional tectonics led to folding and faulting of Methow strata as well as intrabasinal magmatism. Contractional deformation within the Methow basin would have led to uplift and cannibalization of Virginian Ridge and Winthrop Formation deposits, resulting in Turonian and younger deposition of the Ventura member of the Goat Wall unit in angular unconformity with the underlying Virginian Ridge and Winthrop formations. The ages and relative abundance of Jurassic and Cretaceous detrital zircon grains in the overlying Goat Wall unit (Fig. 5) are consistent with previous interpretations that the Ventura member sandstone was derived from cannibalization of the older Virginian Ridge and Winthrop formations, as well as from western sources (McGroder et al. 1990; Garver 1992). Late Cretaceous contraction further deformed the Methow basin, and Paleogene dextral strike-slip displacement segmented the basin into its present configuration.

Early Albian uplift of the magmatic arc east of the Pasayten fault would have provided abundant plutonic sources for the Methow basin, and explain the lack of detrital zircon grains younger than about 104 Ma, even as biostratigraphic constraints suggest deposition occurred through ca. 90 Ma. The variable proportions of Jurassic and Cretaceous ages in the northern and southern portions of the Methow basin may result from a variety of factors, including the following: (*i*) the relative abundance of these ages in sources immediately east of the basin, with more Cretaceous plutons exposed to the north and more Jurassic plutons to the south; (*ii*) differential uplift of sources, with Cretaceous sources experiencing greater uplift in the north than in the south; and (or) (*iii*) complex drainage systems, with a more eastern drainage divide in the north than in the south, permitting a greater contribution of sediment sources within the Cretaceous rocks further east for the northern part of the Methow basin. Although our preferred model of basin evolution requires that the Methow basin was adjacent to its source region in the western Intermontane superterrane, the previous factors and uncertainty in the extent of post-depositional offset along the Pasayten fault precludes identification of specific northern Cretaceous and southern Jurassic plutonic sources within the Jura-Cretaceous arc east of the basin. Because the relative differences in contribution of Cretaceous versus Jurassic sediment persist throughout the Harts Pass and Winthrop formations, these differences do not appear to relate to an increase in Cretaceous sources through the period of deposition.

Assessing extent of post-depositional coast-parallel translation

Wyld et al. (2006) reconstructed the mid-Cretaceous paleogeography of the United States and Canadian Cordillera by restoring known and hypothesized displacements within contractional and extensional belts and along the major strike-slip faults of the northern Cordillera. In what Wyld et al. (2006) refer to as the "minimum offset model", their 100 Ma reconstruction restores the Methow basin 300 km south of its present location, placing the basin northwest of the Blue Mountains Province and hypothesizing a combined Hornbrook–Ochoco–Methow basin that may have shared a common mid-Cretaceous history (Wyld et al. 2006). The "minimum offset model" also shifts terranes of the Intermontane superterrane further south, keeping the Quesnel terrane directly east of the Methow–Tyaughton system, consistent with our provenance results.

A large sedimentary system such as the proposed combined Hornbrook–Ochoco–Methow basin would probably record different provenance signatures for different locations within the basin system, such as a Klamath Mountains source for the Hornbrook Formation in the southwest and a Blue Mountains Province source for the Ochoco basin in the southeast. However, it seems unlikely that there would be no record of mixing of sediment within the larger basin system, particularly in the deeper marine turbidite systems that characterized the mid-Cretaceous Methow, Hornbrook, and Ochoco basins. Mid-Cretaceous strata of the Hornbrook Formation have Early Jurassic and Late Jurassic through Early Cretaceous detrital zircon age peaks, with abundant grains between 150 and 125 Ma and only a handful of grains younger than 130 Ma (Surpless and Beverly 2013). The complete lack of the 120–105 Ma zircon grains in the mid-Cretaceous Hornbrook Formation that are so prominent in the Methow basin, and similarly, the lack of 140–120 Ma grains in the Methow basin that are so common in

Fig. 9. Cartoon block diagrams illustrating model for mid-Cretaceous evolution of the Methow basin. (A) Deposition of the lower and middle Jackass Mountain Group during Early Cretaceous time in a forearc setting with subduction occurring to the west. (B) Sinistral transpression as the outboard Insular superterrane moved >800 km southward resulted in transpression in the Methow region; sinistral and reverse dip-slip motion along the Pasayten fault caused uplift of the magmatic arc rocks intruded into the Intermontane superterrane east of the fault. Transpression also led to uplift of the western margin of the Methow basin, resulting in rapid middle Albian subsidence of the Methow trough and deposition of the east-derived Harts Pass Formation and the west-derived Jackita Ridge Formation and Little Jack unit in the underfilled basin. (C) Cessation of dip-slip motion on the Pasayten fault resulted in dissection of the uplifted highlands east of the basin, permitting fluvial systems to reach further east into the undissected magmatic arc. Continued compression through Turonian time provided abundant west-derived sediment of the Virginian Ridge Formation that interfingered with the east-derived sediment of the Winthrop Formation.

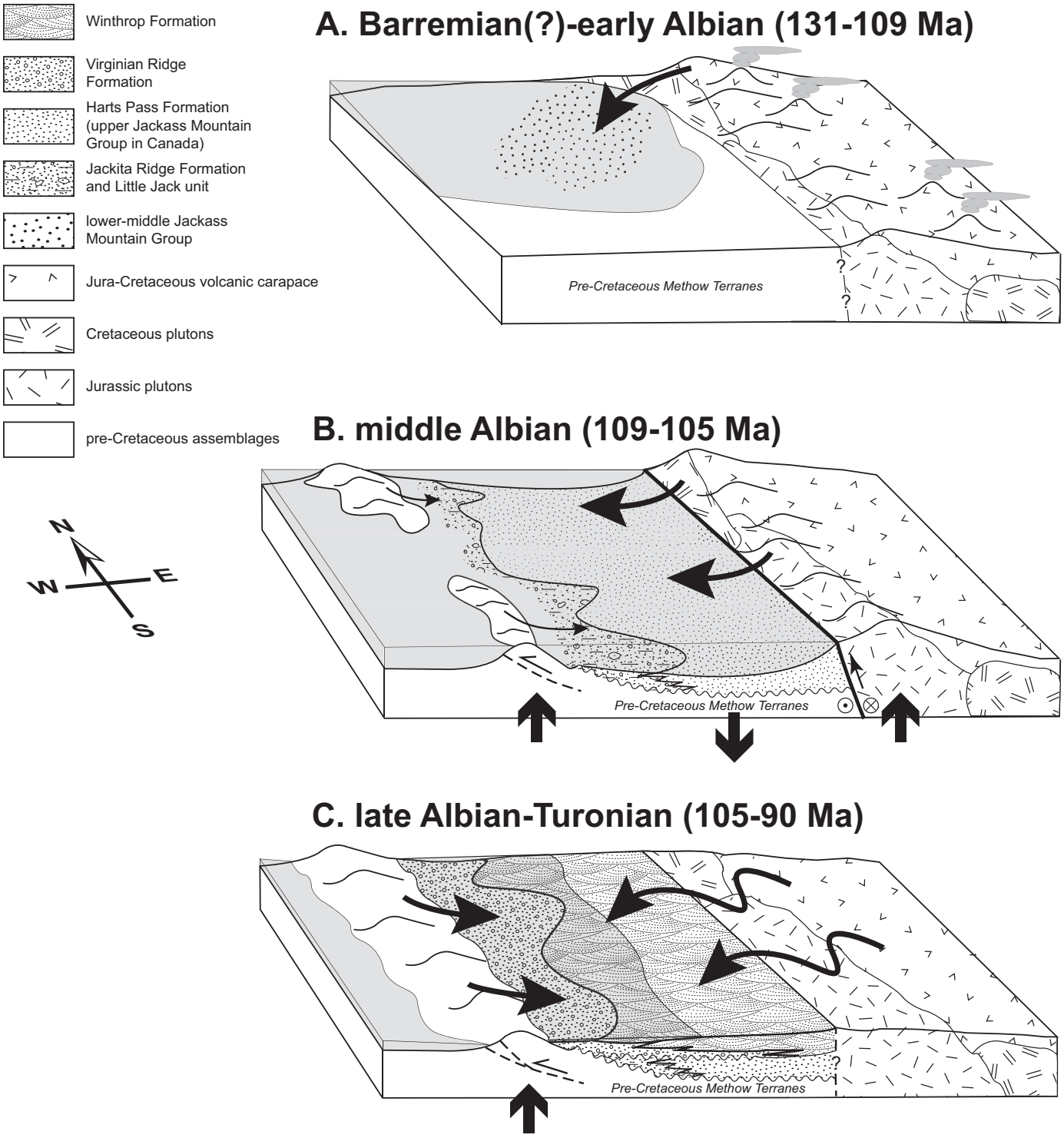

the Hornbrook basin suggests that these were separate systems during the mid-Cretaceous. These two basins also experienced very different tectonic histories, as the mid-Cretaceous history of the Hornbrook basin is one of subsidence rather than compression or transpression, as sedimentation in the Hornbrook basin shifted from alluvial systems in Albian time to shelf and deep basin deposition during Cenomanian through Maastrichtian time (Nilsen 1993; Surpless and Beverly 2013).

Moreover, the Blue Mountains province does not present a likely source region for the Methow basin. Terranes of the Blue Mountains province include a Permian island-arc sequence overlain by Triassic volcanic and volcaniclastic rocks, a Middle to Late Triassic island-arc assemblage containing mostly andesitic volcanic rocks with intercalated sedimentary rocks, disrupted fragments of ocean floor, island-arc volcanic, plutonic, and sedimentary rocks ranging in age from Middle Devonian to Early Jurassic, and a Triassic–Jurassic sedimentary overlap succession that contains abundant Precambrian detrital zircon (Vallier 1995; LaMaskin et al. 2008, 2011; Schwartz et al. 2010). The Blue Mountains Province is intruded by Triassic, Jurassic, and Cretaceous plutons ranging in age from ca. 260 to ca. 160 Ma, ca. 147 Ma, and ca. 115 Ma (Unruh et al. 2008; Anderson et al. 2011; Schwartz et al. 2011). Therefore, although the Blue Mountains Province includes plutonic rocks of Jurassic and Cretaceous age, it also includes a wide range of older plutonic rocks, and detrital zircon derived from the Blue Mountains Province during the mid-Cretaceous would likely reflect this wider range of plutonic ages as well as abundant Precambrian zircon recycled through Triassic and Jurassic cover strata.

The Baja British Columbia hypothesis ("Baja BC" after Irving 1985) suggests that the Intermontane and Insular superterranes accreted to North America much farther south and were translated to their present positions along major dextral strike-slip faults (Champion et al. 1984; Irving 1985; Irving et al. 1985; Irving and Wynne 1990; Cowan et al. 1997; Haggart et al. 2006). In this model, the Insular superterrane would have accreted to North America as far south as present-day Baja California in western Mexico at ca. 100 Ma, and then translated north to join with the Intermontane superterrane after 70 Ma, and then both would have continued north to their present positions in British Columbia (e.g., Irving et al. 1996; Haggart et al. 2006).

The Baja BC hypothesis predicts sediment sources of east-derived strata in the Methow basin would be located in the Peninsular Ranges batholith or Mojave–Sonora region of northern Mexico rather than within the western Intermontane superterrane, but, as previous study of the Methow basin provenance showed (DeGraaff-Surpless et al. 2003), neither of these regions provide a clear match for our Methow basin provenance results. The Peninsular Ranges is generally divided into eastern and western arcs (Johnson et al. 1999) that range in age from 140 to 94 Ma, with the majority of plutons falling between 120 and 95 Ma (George and Dokka 1994; Johnson et al. 1999; Kistler et al. 2003; Ortega-Rivera 2003; Wetmore et al. 2003). The eastern arc is continental in character, with 99–92 Ma tonalitic and granodioritic plutons that have $^{87}Sr/^{86}Sr$ values close to 0.708 (DePaolo 1981; Kimbrough et al. 2001; Kistler et al. 2003), while the western arc includes 140–105 Ma gabbroic to monzogranitic plutons with $^{87}Sr/^{86}Sr \leq 0.704$ and $\varepsilon_{Nd} \geq +3.7$ and a more significant volcanic component than the eastern arc (DePaolo 1981; Johnson et al. 1999; Kimbrough et al. 2001; Todd et al. 2003). The Albian Alisitos Formation is a clastic sedimentary sequence in the western arc of the Peninsular Ranges that contains abundant volcanic lithic grains (Wetmore et al. 2003), unlike the coeval lithic-poor strata of the Harts Pass Formation in the Methow basin. Similarly, the Turonian Vizcaino sandstone of the Peninsular Ranges forearc basin has a large detrital zircon peak at 100–90 Ma tied to the rapidly exhumed 99–92 Ma La Posta suite of the eastern Peninsular Ranges arc (Kimbrough et al. 2001), which is much younger than anything seen in coeval Cenomanian–Turonian strata of the Winthrop Formation in the Methow basin. Neither the eastern nor the western arc of the Peninsular Ranges contains the abundant Jurassic plutons characteristic of the Methow basin provenance.

Although latest Triassic through earliest Cretaceous plutons are common in the Mojave and Sonora regions of southern California and northwest Mexico (Asmerom et al. 1990; Sedlock 2003), they intrude Cambrian to Triassic miogeoclinal strata which overlie several Proterozoic crustal provinces (e.g., Wooden and Miller 1990). The majority of plutonism in the Mojave–Sonora region postdates Methow basin deposition, when granitic plutons intruded into Precambrian basement and Proterozoic–Mesozoic sedimentary sequences during the Laramide Orogeny (90–40 Ma; Valencia-Moreno et al. 2001). $^{87}Sr/^{86}Sr$ values for the region range from 0.703 to 0.706 (Sedlock 2003). Therefore, unlike the provenance record of the Methow basin, mid-Cretaceous sediment derived from this region would likely include a wide range of Mesozoic plutonic ages with variable geochemical signatures, as well as sediment recycled from Paleozoic strata.

Displacement models intermediate to the minimum offset and Baja BC hypotheses place the Methow basin outboard of source regions in the Klamath–Sierran arc as well as the Great Valley Group and Franciscan complex (e.g., Umhoefer 2003; Umhoefer and Blakey 2006). The well-documented magmatic history of the Klamath–Sierran arc includes several distinct pulses during the Early Jurassic through Early Cretaceous (Irwin and Wooden 1999; Allen and Barnes 2006), with the largest volume of plutonism in the Sierra Nevada Mountains occurring between 100 and 85 Ma (Ducea 2001; Irwin 2003). The Cretaceous Great Valley Group is both depositionally and structurally tied to the Klamath–Sierran arc (e.g., Moxon 1990; DeGraaff-Surpless et al. 2002) and mid-Cretaceous Great Valley Group strata display detrital zircon age peaks primarily between 180 and 102 Ma, with a few samples showing nearly unimodal distributions ca. 140–145 Ma (DeGraaff-Surpless et al. 2002). These Great Valley Group detrital zircon signatures do not match the Methow basin provenance signature, making a Klamath–Sierran source for the mid-Cretaceous strata of the Methow basin unlikely.

Our Methow basin provenance results cannot be used to test tectonic models that place both the Intermontane and Insular superterrane together at southern latitudes (e.g., Enkin et al. 2006). Our results are consistent with previous studies that suggest Methow provenance within the western Intermontane superterrane, along with the westernmost Okanogan Range (e.g., DeGraaff-Surpless et al. 2003), but cannot preclude the possibility that both the eastern Coast Mountains batholith and the Intermontane superterrane into which it intrudes were also located further south. The lack of abundant Precambrian detrital zircon in the Methow strata prevents any definitive links between the Methow basin and specific regions of the North American craton. Given the likelihood of zircon recycling and homogenization of Precambrian detrital zircon through time (cf. LaMaskin et al. 2011), reliance on Precambrian detrital zircon ages alone is unlikely to resolve the translation debate.

Conclusions

Detailed provenance analysis of the east-derived, mid-Cretaceous strata of the Methow basin reveals a remarkably uniform source signature dominated by Jurassic and Cretaceous plutonic and volcanic rocks. The eastern belt of the Coast Mountains batholith that intruded into the Intermontane superterrane in two magmatic flux events at ca. 160 and 120–110 Ma (Gehrels et al. 2009), combined with Jurassic and Cretaceous plutons in the westernmost Okanogan Range, represent the most likely sediment sources for east-derived Methow strata, given their proximity and matching ages, compositions, and geochemistry. Our results suggest that mid-Cretaceous deposition in the Methow basin began in

a sinistral transpressional setting, with reverse faulting along a northwest-striking Pasayten fault, resulting in uplift of the adjacent highlands east of the fault. Transpression also uplifted the western margin of the basin beginning in middle Albian, leading to maximum subsidence of the Methow trough and rapid deposition of the east-derived Harts Pass Formation. Eastern uplift and subsidence of the Methow basin ended by late Albian as uplift of the western margin continued, resulting in west-derived Virginian Ridge sedimentation and east-derived Winthrop Formation sedimentation in shallow marine and nonmarine systems. With increasing dissection of the magmatic arc east of the basin, the drainage divide shifted further east, adding volcanic sediment derived from the undissected eastern arc to Methow basin strata during Winthrop Formation deposition. Following deposition of the Winthrop Formation and the younger volcanic Goat Wall unit within the basin, regional contraction led to intrabasinal thrust faulting and closure of the Methow basin. Our provenance results are consistent with tectonic models that place the Cretaceous Methow basin directly west of the eastern belt of the Coast Mountains batholith and the Okanogan Range, but do not preclude potential large-scale translation of both the Methow basin together with its proximal eastern sources along a hypothetical fault system located somewhere east of the Methow basin sources that were within the western Intermontane superterrane.

Acknowledgements

The authors are grateful for the extensive field and laboratory assistance provided by Brant Konetchy, Aaron Price, and Stephen Muela. The authors wish to thank George Gehrels, Mark Pecha, Nicky Giesler, and Clayton Loehn at the University of Arizona LaserChron Center for their assistance with detrital zircon U–Pb and Lu–Hf sample preparation, imaging, analysis, and data processing, and we gratefully acknowledge NSF-EAR 1032156 for support of the Arizona LaserChron Center. We thank the GeoAnalytical Lab at Washington State University for all major- and trace-element geochemical data. Constructive reviews from Associate Editor Graham Andrews and an anonymous reviewer greatly improved this manuscript. This research was funded by a Trinity University Mach Research Scholarship awarded to T. Koplitz and NSF-EAR-ICER 846695 awarded to K.D. Surpless.

References

Allen, C.M., and Barnes, C.G. 2006. Ages and some cryptic sources of Mesozoic plutonic rocks in the Klamath Mountains, California and Oregon. *In* Geological Studies in the Klamath Mountains province, California and Oregon: A volume in honor of William P. Irwin. *Edited by* A.W. Snoke and C.G. Barnes. Geological Society of America Special Paper, **410**: 223–245.

Amelin, Y., Lee, D.C., Halliday, A.N., and Pidgeon, R.T. 1999. Nature of the Earth's earliest crust from hafnium isotopes in single detrital zircons. Nature, **399**: 252–255. doi:10.1038/20426.

Anderson, B.S., Schwartz, J.J., Johnson, K., Wooden, J.L., and Mueller, P.A. 2011. U-Pb Geochronology and Hf Isotope Geochemistry of the Mountain HomeMetamorphic Complex, Blue Mountains Province, northeastern Oregon. Geological Society of America Abstracts with Programs, **43**: 76.

Armstrong, R.L. 1988. Mesozoic and early Cenozoic magmatic evolution of the Canadian Cordillera, *In* Processes in continental lithospheric deformation. *Edited by* S.P. Clark, B.B. Burchfiel, and J. Suppe. Geological Society of America Special Paper, **218**: 55–91.

Asmerom, Y., Zartman, R.E., Damon, P.E., and Shafiqullah, M. 1990. Zircon U-Th-Pb and whole-rock Rb-Sr age patterns of the lower Mesozoic igneous rocks in the Santa Rita Mountains, southeast Arizona: Implications for Mesozoic magmatism and tectonics in the southern Cordillera. Geological Society of America Bulletin, **102**: 961–968. doi:10.1130/0016-7606(1990)102<0961:ZUTPAW>2.3.CO;2.

Barfod, D.N., and Nelson, B.K. 1992. Isotopic evidence for provenance of Mesozoic sediments of the Methow Basin, Washington and British Columbia. Abstracts with Programs – Geological Society of America, **24**: 5.

Barksdale, J.D. 1975. Geology of the Methow Valley, Okanogan County, Washington: Washingon Division of Geology and Earth Resources Bulletin, **68**: 72.

Bracciali, L., Marroni, M., Pandolfi, L., and Rocchi, S. 2007. Geochemistry and petrography of Western Tethys Cretaceous sedimentary covers (Corsica and Northern Appennines): From source areas to configuration of margins, *In* Sedimentary provenance and petrogenesis: Perspectives from petrography and Geochemistry. *Edited by* J. Arribas, S. Critelli, and M. Johnson. Geological Society of America Special Paper **420**: 73–93.

Butler, R.F., Gehrels, G.E., McClelland, W.C., May, S.R., and Klepacki, D. 1989. Discordant paleomagnetic poles from the Canadian Coast Plutonic Complex: Regional tilt rather than large-scale displacement? Canadian Journal of Geosciences, **17**: 691–694.

Butler, R.F., Gehrels, G.E., and Kodama, K.P. 2001. A Moderate Translation Alternative to the Baja British Columbia Hypothesis. GSA Today, **11**: 4–10. doi:10.1130/1052-5173(2001)011<0004:ALFTCI>2.0.CO;2.

Carr, S.D. 1991. U-Pb zircon and titanite ages of three Mesozoic igneous rocks south of the Thor-Odin-Pinnacles area, southern Omineca Belt, British Columbia. Canadian Journal of Earth Sciences, **28**(12): 1887–1882. doi:10.1139/e91-171.

Carr, S.D. 1995. The southern Omineca Belt, British Columbia: new perspectives from the Lithoprobe Geoscience Program. Canadian Journal of Earth Sciences, **32**(10): 1720–1739. doi:10.1139/e95-135.

Cecil, R.M., Gehrels, G., Ducea, M.N., and Patchett, P.J. 2011. U-Pb-Hf characterization of the central coast Mountains batholith: Implications for petrogenesis and crustal architecture. Lithosphere, **3**: 247–260. doi:10.1130/L134.1.

Champion, D.E., Howell, D.G., and Gromme, C.S. 1984. Paleomagnetic and geological data indicating 2500 km of northward displacement for the Salinian and related terranes, California. Journal of Geophysical Research, **89**: 7736–7752. doi:10.1029/JB089iB09p07736.

Coates, J.A. 1974. Geology of the Manning Park area, British Columbia. Geological Survey of Canada Bulletin, **238**: 177 p.

Cole, M.R. 1973. Petrology and dispersal patterns of Jurassic and Cretaceous sedimentary rocks in the Methow river area, North Cascades, Washington. Ph.D. thesis. University of Washinton, Seattle, Washington, U.S.

Cowan, D.S., Brandon, M.T., and Garver, J.I. 1997. Geological Tests of Hypotheses For Large Coastwise Displacements-A Critique Illustrated By The Baja British Columbia Controversy. American Journal of Science, **297**: 117–173. doi:10.2475/ajs.297.2.117.

Cox, R., Donald, R.L., and Cullers, R.L. 1995. The influence of sediment recycling and basement composition on evolution of mudrock chemistry in the southwestern United States. Geochimica et Cosmochimica Acta, **59**: 2919–2940. doi:10.1016/0016-7037(95)00185-9.

DeGraaff-Surpless, K., Graham, S.A., Wooden, J.L., and McWilliams, M.O. 2002. Detrital zircon provenance analysis of the Great Valley Group, California: Evolution of an arc-forearc system. Geological Society of America Bulletin, **114**: 1564–1580. doi:10.1130/0016-7606(2002)114<1564:DZPAOT>2.0.CO;2.

DeGraaff-Surpless, K., Mahoney, J.B., Wooden, J.L., and McWilliams, M.O. 2003. Lithofacies control in detrital zircon provenance studies: Insights from the Cretaceous Methow basin, southern Canadian Cordillera. Geological Society of America Bulletin, **115**: 899–915. doi:10.1130/B25267.1.

DePaolo, D.J. 1981. A neodymium and strontium isotopic study of Mesozoic calc-alkaline granitic batholiths of the Sierra Nevada and Peninsular Ranges, California. Journal of Geophysical Research, **86**: 10470–10488. doi:10.1029/JB086iB11p10470.

Dickinson, W.R. 1970. Interpreting Detrital Modes of Greywacke and Arkose. Journal of Sedimentary Petrology, **40**: 695–707. doi:10.1306/74D72018-2B21-11D7-8648000102C1865D.

Dickinson, W.R., Beard, S.L., Brakenridge, R.G., Erjavec, J.L., Ferguson, R.C., Inman, K.F., Knepp, R.A., Lindberg, A.F., and Ryberg, P.T. 1983. Provenance of North American Phanerozoic sandstones in relation to tectonic setting. Geological Society of America Bulletin, **94**: 222–235. doi:10.1130/0016-7606(1983)94<222:PONAPS>2.0.CO;2.

Dorsey, R.J., and Lenegan, R.J. 2007. Structural controls on Middle Cretaceous sedimentation in the Toney Butte area of the Mitchell Inlier, Ochoco Basin, central Oregon. Geological Society of America Special Paper, **419**: 97–115. doi:10.1130/2006.2419(05).

Ducea, M. 2001. The California Arc: thick Granitic Batholiths, Eclogitic Residues, Lithosperic-Scale Thrusting and Magmatic Flare-Ups. GSA Today, **11**: 4–10. doi:10.1130/1052-5173(2001)011<0004:ALFTCI>2.0.CO;2.

Enkin, R.J., Mahoney, J.B., Baker, J., Kiessling, M., and Haugerud, R.A. 2002. Syntectonic remagnetization in the southern Methow block: Resolving large displacements in the southern Canadian Cordillera. Tectonics, **21**: 18. doi:10.1029/2001TC001294.

Enkin, R.J., Mahoney, B.J., and Baker, J. 2006. Paleomagnetic signature of the Silverquick/Powell Creek succession, south-central British Columbia; reaffirmation of Late Cretaceous large-scale terrane translation. *In* Paleogeography of the North American Cordillera: Evidence For and Against Large-Scale Displacements. *Edited by* J.W. Haggart, R.J. Enkin, and J.W.H Monger. Geological Association of Canada Special Paper, **46**: 201–218.

Erdmer, P., Heaman, L., Creaser, R.A., Thompson, R.I., and Daughtry, K.L. 2001. Eocambrian granite clasts in southern British Columbia shed light on Cordilleran hinterland crust. Canadian Journal of Earth Sciences, **38**(7): 1007–1016. doi:10.1139/e01-005.

Ewart, A. 1982. The mineralogy and petrology of Tertiary-Recent orogenic volcanic rocks: with special reference to the andesitic-basaltic compositional range, *in* Thorpe, R.S., ed., Andesites: Orogenic andesites and related rocks: Chichester, U.K., John Wiley & Sons, pp. 25–95.

Fiet, N., Beaudoin, B., and Parize, O. 2001. Lithostratigraphic analysis of Milankovitch cyclicity in pelagic Albian deposits of central Italy: implications for the

duration of the stage and substages. Cretaceous Research, **22**: 265–275. doi:10.1006/cres.2001.0258.

Garver, J.I. 1989. Basin evolution and source terranes of Albian-Cenomanian rocks in the Tyaughton Basin, southern British Columbia; implications for Mid-Cretaceous tectonics in the Canadian Cordillera. Ph.D. thesis, University of Washington, Seattle, Washington, U.S.

Garver, J.I. 1992. Provenance of Albian-Cenomanian rocks of the Methow and Tyaughton basins, southern British Columbia: a mid-Cretaceous link between North America and the Insular terrane. Canadian Journal of Earth Sciences, **29**(6): 1274–1295. doi:10.1139/e92-102.

Garver, J.I., and Brandon, M.T. 1994. Fission-track ages of detrital zircons from Cretaceous strata, southern British Columbia: Implications for the Baja BC hypothesis. Tectonics, **13**: 401–420. doi:10.1029/93TC02939.

Garver, J.I., and Royce, P.R. 1993. Chromium and nickel in shale of the foreland deposits of the Ordovician Taconic Orogeny; using shale as a provenance indicator for ultramafic rocks. Abstracts with Programs – Geological Society of America, **25**: 17.

Garver, J.I., and Scott, J.T. 1995. Trace elements in shale as indicators of crustal provenance and terrane accretion in the southern Canadian Cordillera. Geological Society of America Bulletin, **107**: 440–453. doi:10.1130/0016-7606(1995)107<0440:TEISAI>2.3.CO;2.

Garver, J.I., Heller, P.L., and Jett, G.A. 1988. Tectonic significance of polymodal compositions in mélange sandstones, Western Melange Belt, North Cascade Range, Washington; discussion and reply. Journal of Sedimentary Petrology, **58**: 1046–1050.

Garver, J.I., Royce, P.R., and Scott, T.J. 1994. The presence of ophiolites in tectonic highlands as determined by chromium and nickel anomalies in synorogenic shale: Two examples from North America. Geologiya i Geofizika, **35**: 3–11.

Gehrels, G., Valencia, V., and Pullen, A. 2006. Detrital Zircon Geochronology by Laser Ablation Multicollector ICPMS at the Arizona LaserChron Center. *In* Geochronology: Emerging Opportunites. *Edited by* T. Olszewski. Paleontology Society Papers, **12**: 67–76.

Gehrels, G., Valencia, V., and Ruiz, J. 2008. Enhanced precision, accuracy, efficiency, and spatial resolution of U-Pb ages by laser ablation-multicollector-inductively coupled plasma-mass spectrometry [online]. Geochemistry, Geophysics, Geosystems, **9**: Q03017. doi:10.1029/2007GC001805.

Gehrels, G., Rusmore, M., Woodsworth, G., Crawford, M., Andronicos, C., Hollister, L., Pathchett, J., Ducea, M., Butler, R., Klepeis, K., Davidson, C., Friedman, R., Haggart, J., Mahoney, B., Crawford, W., Pearson, D., and Girardi, J. 2009. U-Th-Pb geochronology of the Coast Mountains batholith in north-coastal British Columbia: Constraints on age and tectonic evolution. Geological Society of America Bulletin, **121**: 1341–1361. doi:10.1130/B26404.1.

George, R.G., and Dokka, R.K. 1994. Major Late Cretaceous cooling events in the eastern Peninsular Ranges, California, and their implication for Cordilleran tectonics. Geological Society of America Bulletin, **106**: 903–914. doi:10.1130/0016-7606(1994)106<0903:MLCCEI>2.3.CO;2.

Girty, G.H., Barber, R.W., and Knaack, C. 1993. REE, Th, and Sc evidence for the depositional setting and source rock characteristics of the Quartz Hill Chert, Sierra Nevada, California, *in*, Johnsson, M.J., and Basu, A., eds., Processes controlling the composition of clastic sediments, Geological Society of America Special Paper, v. 284, pp. 109–119.

Grieg, C.J. 1992. Jurassic and Cretaceous plutonic and structural styles of the Eagle Plutonic Complex, southwestern British Columbia, and their regional significance. Canadian Journal of Earth Sciences, **29**(4): 793–811. doi:10.1139/e92-067.

Grieg, C.J., Armstrong, R.L., Harakal, J.E., Runkle, D., and Van der Heyden, P. 1992. Geochronometry of the Eagle Plutonic Complex and the Coquihalla area, southwestern British Columbia. Canadian Journal of Earth Sciences, **29**(4): 812–829. doi:10.1139/e92-068.

Gromet, L.P., and Silver, L.T. 1987. REE variations across the Peninsular Ranges Batholith; implications for batholithic petrogenesis and crustal growth in magmatic arcs. Journal of Petrology, **28**: 75–125. doi:10.1093/petrology/28.1.75.

Haggart, J.W., Enkin, R.J., and Monger, J.W.H. 2006. Strengths and limitations of paleogeographic methods in assessing large-scale displacements within the North American Cordillera. *In* Paleogeography of the North American Cordillera: Evidence For and Against Large-Scale Displacements. *Edited by* J.W. Haggart, R.J. Enkin, and J.W.H. Monger. Geological Association of Canada Special Paper, **46**: 1–11.

Haugerud, R.A., Mahoney, J.B., and Dragovitch, J.D. 1996. Geology of the Methow block: Northwest Geological Society, Fall Field Trip, Guidebook. Seattle, Washington, Northwest Geological Society. 37 p.

Hoskin, P.W.O., and Schaltegger, U. 2003. The Composition of zircon and igneous and metamorphic petrogenesis. *In* Zircon. *Edited by* J.M. Hanchar and P.W.O. Hoskin. Reviews in Mineralogy & Geochemistry, **53**: 27–62.

Hurlow, H.A. 1993. Mid-Cretaceous strike-slip and contractional fault zones in the western intermontane terrane, Washington, and their relation to the North Cascades-southeastern Coast Belt orogen. Tectonics, **12**: 1240–1257. doi:10.1029/93TC01061.

Hurlow, H.A., and Nelson, B.K. 1993. U-Pb zircon and monazite ages for the Okanogan Range Batholith, Washington: Implications for the Magmatic and tectonic evolution of the southern Canadian and northern United States Cordillera. Geological Society of America Bulletin, **107**: 231–240.

Irving, E. 1985. Whence British Columbia? Nature, **314**: 673–674. doi:10.1038/314673a0.

Irving, E., and Wynne, P.J. 1990. Paleomagnetic evidence bearing on the evolution of the Canadian Cordillera. Philosophical Transactions of the Royal Society of London, **A331**: 487–509.

Irving, E., Woodsworth, G.J., Wynne, P.J., and Morrison, A. 1985. Paleomagnetic evidence for displacement from the south of the Coast Plutonic Complex, British Columbia. Canadian Journal of Earth Sciences, **22**(4): 584–598. doi:10.1139/e85-058.

Irving, E., Wynne, P.J., Thorkelson, D.J., and Schiarizza, P. 1996. Large (1000 to 4000 km) northward movements of tectonic domains in the northern Cordillera, 83 to 45 Ma. Journal of Geophysical Research, **101**: 17901–17916. doi:10.1029/96JB01181.

Irwin, W.P. 2003. Correlation of the Klamath Mountains and Sierra Nevada. U.S. Geological Survey Open-File Report 02-490.

Irwin, W.P., and Wooden, J.L. 1999. Plutons and accretionary episodes of the Klamath Mountains, California and Oregon. U.S. Geological Survey Open-File Report 99-0374.

Johnson, S.E., Tate, M.C., and Fanning, M.C. 1999. New geologic mapping and SHRIMP U-Pb zircon data in the Peninsular Ranges batholith, Baja California, Mexico. Evidence for a suture?. Geology, **27**: 743–746. doi:10.1130/0091-7613(1999)027<0743:NGMASU>2.3.CO;2.

Kiessling, M.A. 1998. Provenance and stratigraphic correlation of the mid-Cretaceous Pasayten Group, northern Washington and Manning Provincial Park, British Columbia. M.S. Thesis, Idaho State University, 148 p.

Kiessling, M.A., and Mahoney, J.B. 1997. Revised stratigraphy of the Pasayten Group, Manning Park, British Columbia. Current Research 1997-A, Geological Survey of Canada, pp. 151–158.

Kimbrough, D.L., Smith, D.P., Mahoney, J.B., Moore, T.E., Grove, M., Gastil, R.G., Ortega-Rivera, A., and Fanning, C.M. 2001. Forearc-basin sedimentary response to rapid Late Cretaceous batholith emplacement in the Peninsular Ranges of southern and Baja California. Geology, **29**: 491–494. doi:10.1130/0091-7613(2001)029<0491:FBSRTR>2.0.CO;2.

Kinny, P.D., and Maas, R. 2003. Lu-Hf and Sm-Nd isotope systems in zircon. *In* Zircon. *Edited by* J.M. Hanchar and P.W.O. Hoskin. Reviews in Mineralogy and Geochemistry, **53**: 327–335.

Kistler, R.W., Wooden, J.L., and Morton, D.M. 2003. Isotopes and ages in the northern Peninsular Ranges batholith, southern California: U.S. Geological Survey Open-File Report 03-0489. 45 p.

Kleinspehn, K.L. 1982. Cretaceous sedimentation and tectonics, Tyaughton-Methow Basin, southwestern British Columbia. Ph.D. thesis, Princeton University, Princeton, New Jersey, U.S.

Kleinspehn, K.L. 1985. Cretaceous sedimentation and tectonics, Tyaughton-Methow Basin, southwestern British Columbia. Candian Journal of Earth Sciences, **22**(2): 154–174. doi:10.1139/e85-014.

Knaack, C., Cornelius, S., and Hooper, P. 1994. Trace element analyses of rocks and minerals by ICP-MS. Open File Report, Washington State University, Pullman, Washington, U.S.

Kodama, K.P., and Ward, P.D. 2001. Compaction-corrected paleomagnetic paleolatitudes for Late Cretaceous rudists along the Cretaceous California margin; evidence for less than 1500 km of post-Late Cretaceous offset for Baja British Columbia, **113**: 1171–1178. doi:10.1130/0016-7606(2001)113<1171:CCPPFL>2.0.CO;2.

LaMaskin, T.A., Dorsey, R.J., and Vervoot, J.D. 2008. Tectonic controls on mudrock geochemistry, Mesozoic rocks of eastern Oregon and western Idaho, U.S.A.; implications for Cordillera tectonics. Journal of Sedimentary Research, **78**: 765–783. doi:10.2110/jsr.2008.087.

LaMaskin, T.A., Vervoort, J.D., Dorsey, R.J., and Wright, J.E. 2011. Early Mesozoic paleogeography and tectonic evolution of the Western United States: Insights from detrital zircon U-Pb geochronology, Blue Mountains Province, northeastern Oregon. Geological Society of America Bulletin, **123**: 1939–1965. doi:10.1130/B30260.1.

Lawrence, R.D. 1978. Tectonic significance of petrofabric studies along the Chewack-Pasayten Fault, North-central Washington. Geological society of America Bulletin, **89**: 731–743. doi:10.1130/0016-7606(1978)89<731:TSOPSA>2.0.CO;2.

Li, Y.H. 2000. A compendium of geochemistry: Princeton, New Jersey, Princeton University Press, 475 p.

Ludwig, K. 2008. Isoplot 3.6. Berkeley Geochronology Center Special Publication 4. 77 p.

MacLaurin, C.I., Mahoney, J.B., Haggart, J.W., Goodin, J.R., and Mustard, P.S. 2011. The Jackass Mountain Group of south-central British Columbia: depositional setting and evolution of an Early Cretaceous deltaic complex. Canadian Journal of Earth Science, **48**(6): 930–951. doi:10.1139/e11-035.

Mahoney, B.J. 1994. Nd isotopic signatures and stratigraphic correlations; examples from western Pacific marginal basins and Middle Jurassic rocks of the southern Canadian Cordillera. Ph.D. thesis, University of British Columbia, Vancouver, B.C.

McClelland, W.C., Gehrels, G.E., and Saleeby, J.B. 1992. Upper Jurassic-Lower Cretaceous basinal strata along the Cordilleran margin: implications for the accretionary history of the Alexander-Wrangellia-Peninsular terrane. Tectonics, **11**: 823–835. doi:10.1029/92TC00241.

McGroder, M.F., Garver, J.L., and Mallory, V.S. 1990. Bedrock geologic map, biostratigraphy and structure sections of the Methow Basin, Washington and

British Columbia. Open-File Report, Washington State Division of Geology and Earth Resources, Olympia, Washington, U.S.

McLennan, S.M., Taylor, S.R., McCulloch, M.T., and Maynard, J.B. 1990. Geochemical and Nd-Sr isotopic composition of deep-sea turbidites; crustal evolution and plate tectonic associations. Geochimica et Cosmochimica Acta, **54**: 2015–2050. doi:10.1016/0016-7037(90)90269-Q.

McLennan, S.M., Hemming, S., McDaniel, D.K., and Hanson, G.N. 1993. Geochemical approaches to sedimentation, provenance, and tectonics. Geological Society of America Special Paper, **284**: 21–40. doi:10.1130/SPE284-p21.

McLennan, S.M., Bock, B., Hemming, S.R., Hurowitz, J.A., Lev, S.M., and McDaniel, D.K. 2003. The roles of provenance and sedimentary processes in the geochemistry of sedimentary rocks. *In* Geochemistry of Sediments and Sedimentary Rocks: Evolutionary Considerations to Mineral Deposit-Forming Environments. *Edited by* D.R. Lentz. Geological Association of Canada, GeoText **4**: 7–38.

Miller, I.M., Brandon, M.T., and Hickey, L.J. 2006. Using leaf margin analysis to estimate the mid-Cretaceous (Albian) paleolatitude of the Baja BC block. Earth and Planetary Science Letters, **245**: 95–114. doi:10.1016/j.epsl.2006.02.022.

Monger, J.W.H. 1970. Hope map-area, west half (92hw1/2), british columbia. Geological Survey of Canada, Ottawa, Ont., Canada.

Monger, J.W.H., Price, R.A., and Tempelman-Kluit, D.J. 1982. Tectonic accretion and the origin of the two major metamorphic and plutonic welts in the Canadian Cordillera. Geology, **10**: 70–75. doi:10.1130/0091-7613(1982)10<70:TAATOO>2.0.CO;2.

Monger, J.W.H., van der Hayden, P., Journeay, J.M., Evenchick, C.A., and Mahoney, J.B. 1994. Jurassic-Cretaceous basins along the Canadian Coast Belt: Their bearing on pre-mid-Cretaceous sinistral displacements. Geology, **22**: 175–178. doi:10.1130/0091-7613(1994)022<0175:JCBATC>2.3.CO;2.

Moxon, I.W. 1990. Stratigraphic and structural architecture of the San Joaquin-Sacramento Basin. Ph.D. Stanford University. 371 p.

Nesbitt, H.W., and Young, G.M. 1982. Early Proterozoic climates and plate motions inferred from major element chemistry of lutites. Nature, **299**: 715–717. doi:10.1038/299715a0.

Nilsen, T.H. 1993. Stratigraphy of the Cretaceous Hornbrook Formation, Southern Oregon and Northern California. U.S. Geological Survey Professional Paper, p. 1–89.

Ortega-Rivera, A. 2003. Geochronological constraints on the tectonic history of the Peninsular Ranges batholith of Alta and Baja California: Tectonic Implications for western Mexico. *In* Tectonic evolution of northwestern Mexico and the southwestern USA. *Edited by* S.E. Johnson, S.R. Paterson, J.M. Fletcher, G.H. Girty, D.L. Kimbrough, and A. Martín-Barajas. Geological Society of America Special Paper, **374**: 297–335.

Pearce, J.A. 1983. Role of sub-continental lithosphere in magma genesis at active continental margins. *In* Continental Basalts and Mantle Xenoliths. *Edited by* C.J. Hawkesworth and M.J. Norry. Shiva Publishing Limited, Nantwich, U.K. pp. 230–249.

Petö, P. 1974. Plutonic Evolution of the Canadian Cordillera. Geological Society of America Bulletin, **85**: 1269–1276. doi:10.1130/0016-7606(1974)85<1269:PEOTCC>2.0.CO;2.

Petö, P., and Armstrong, R.L. 1976. Strontium isotope study of the composite batholith between Princeton and Okanagan Lake. Canadian Journal of Earth Sciences, **13**(11): 1577–1583. doi:10.1139/e76-164.

Plank, T., and Langmuir, C.H. 1998. The chemical composition of subducting sediment and its consequences for the crust and mantle. Chemical Geology, **145**: 325–394. doi:10.1016/S0009-2541(97)00150-2.

Potter, P.E., Maynard, J.B., and Depetris, P.J. 2005. Mud and Mudstones: Introduction and Overview. Springer, New York, U.S.

Ray, G.E. 1990. The geology and mineralization of the Coquihalla gold belt and Hozameen fault system, southwestern British Columbia (92H/6, 11, 14). B.C. Ministry of Energy, Mines and Petroleum Resources, **79**.

Ross, G.M., and Parrish, R.R. 1991. Detrital zircon geochronology of metasedimentary rocks in the southern Omineca Belt, Canadian Cordillera. Canadian Journal of Earth Sciences, **28**(8): 1254–1270. doi:10.1139/e91-112.

Schwartz, J.J., Snoke, A.W., Frost, C.D., Barnes, C.G., Gromet, L.P., and Johnson, K. 2010. Analysis of the Wallowa-Baker terrane boundary: Implications for tectonic accretion in the Blue Mountains province, northeastern Oregon. Geological Society of America Bulletin, **122**: 517–536. doi:10.1130/B26493.1.

Schwartz, J.J., Snoke, A.W., Cordey, F., Johnson, K., Frost, C.D., Barnes, C.G., LaMaskin, T.A., and Wooden, J.L. 2011. Late Jurassic magmatism, metamorphism, and deformation in the Blue Mountains Province, northeast Oregon: Geological Society of America Bulletin, **123**: 2083–2111.

Sedlock, R.L. 2003. Geology and tectonics of the Baja California peninsula and adjacent areas, *In* Tectonic evolution of northwestern Mexico and the southwestern USA. *Edited by* S.E. Johnson, S.R. Paterson, J.M. Fletcher, G.H. Girty, D.L. Kimbrough, and A. Martín-Barajas. Geological Society of America Special Paper, **374**: 1–42.

Surpless, K.D., and Beverly, E.J. 2013. Understanding a critical basinal link in Cretaceous Cordilleran paleogeography; detailed provenance of the Hornbrook Formation, Oregon and California. Geological Society of America Bulletin, **125**: 709–727. doi:10.1130/B30690.1.

Taylor, S.R., and McLennan, S.M. 1985. Continental Crust: its composition and Evolution. Blackwell Scientific Publications, Oxford, U.K.

Tennyson, M.E., and Cole, M.R. 1978. Tectonic significance of upper Mesozoic-Pasayten sequence, northeastern Cascade Range, Washington and British Columbia, *In* Mesozoic paleogeography of the western United States: Los Angeles, Pacific section. *Edited by* A.G. Howell, and K. Mcdougall. Pacific Coast Paleogeography Symposium, Society of Economic Paleontologists and Mineralogists, **2**: 499–508.

Thorkelson, D.J., and Smith, A.D. 1989. Arc and intraplate volcanism in the Spences Bridge Group; implications for Cretaceous tectonics in the Canadian Cordillera. Geology, **17**: 1093–1096. doi:10.1130/0091-7613(1989)017<1093:AAIVIT>2.3.CO;2.

Todd, V.R., Shaw, S.E., and Hammarstrom, J.M. 2003. Cretaceous plutons of the Peninsular Ranges batholith, San Diego and westernmost Imperial Counties, California: Intrusion across a Late Jurassic continental margin. *In* Tectonic evolution of northwestern Mexico and the southwestern USA. *Edited by* S.E. Johnson, S.R. Paterson, J.M. Fletcher, G.H. Girty, D.L. Kimbrough, and A. Martín-Barajas. Geological Society of America Special Paper, **374**: 185–235.

Trexler, J.H., Jr., and Bourgeois, J. 1985. Evidence For Mid-Cretaceous Wrench-Faulting In The Methow Basin, Washington: Tectonostratigraphic Setting Of The Virginia Ridge Formation. Tectonics, **4**: 379–394. doi:10.1029/TC004i004p00379.

Umhoefer, P.J. 2003. A model for the North America Cordillera in the Early Cretaceous: Tectonic escape related to arc collision of the Guerrero terrane and a change in North American plate motion. *In* Tectonic evolution of northwestern Mexico and the southwestern USA. *Edited by* S.E. Johnson, S.R. Paterson, J.M. Fletcher, G.H. Girty, D.L. Kimbrough, and A. Martín-Barajas. Geological Society of America Special Paper, **374**: 117–134.

Umhoefer., P.J., and Blakey, R.C. 2006. Moderate (1600 km) northward translation of Baja British Columbia from Southern California; an attempt at reconciliation of paleomagnetism and geology. Geological Association of Canada Special Paper, **46**: 307–329.

Umhoefer, P.J., and Schiarizza, P. 1996. Latest Cretaceous to early Tertiary dextral strike-slip faulting on the southeastern Yalakom fault system, southeastern Coast Belt, British Columbia. Geological Society of America Bulletin, **108**: 768–785. doi:10.1130/0016-7606(1996)108<0768:LCTETD>2.3.CO;2.

Unruh, D.M., Lund, Karen, Kuntz, M.A., and Snee, L.W. 2008. Uranium-lead zircon ages and Sr, Nd, and Pb isotope geochemistry of selected plutonic rocks from western Idaho. U.S. Geological Survey Open-File Report 2008-1142: 37 p.

Valencia-Moreno, M., Ruiz, J., Barton, M.D., Patchett, J.P., Zürcher, L., Hodkinson, D.G., and Roldan-Quintana, J. 2001. A chemical and isotopic study of the Laramide granitic belt of northwestern Mexico: Identification of the southern edge of the North American Precambrian basement. Geological Society of America Bulletin, **113**: 1409–1422. doi:10.1130/0016-7606(2001)113<1409:ACAISO>2.0.CO;2.

Vallier, T.L. 1995. Petrology of pre-Tertiary igneous rocks in the Blue Mountains region of Oregon, Idaho, and Washington: implications for the geologic evolution of a complex island arc. *In* Geology of the Blue Mountains region of Oregon, Idaho, and Washington: Petrology and Tectonic Evolution of Pre-Tertiary Rocks of the Blue Mountains Region. *Edited by* T.L. Vallier and H.C. Brooks. U.S. Geological Survey, Professional Paper, **1438**: 125–209.

Vervoort, J.D., and Bichert-Toft, J. 1999. Evolution of the depleted mantle; Hf isotope evidence from juvenile rocks through time. Geochimica et Cosmochimica Acta, **63**: 533–566. doi:10.1016/S0016-7037(98)00274-9.

Ward, P.D., Hurtado, J.M., Kirschvink, J.L., and Verosub, K.L. 1997. Measurements of the Cretaceous Paleolatitude of Vancouver Island: Consistent with the Baja-British Columbia Hypothesis. Science, **277**: 1642–1645. doi:10.1126/science.277.5332.1642.

Wetmore, P.H., Herzig, C., Alsleben, H., Sutherland, M., Schmidt, K.L., Schultz, P.W., and Paterson, S.R. 2003, Mesozoic tectonic evolution of the Peninsular Ranges of southern and Baja California. *In* Tectonic evolution of northwestern Mexico and the southwestern USA. *Edited by* S.E. Johnson, S.R. Paterson, J.M. Fletcher, G.H. Girty, D.L. Kimbrough, and A. Martín-Barajas. Geological Society of America Special Paper, **374**: 93-116.

Wooden, J.L., and Miller, D.M. 1990. Chronologic and isotopic framework for Early Proterozoic crustal evolution in the eastern Mojave Desert region, SE California. Journal of Geophysical Research, **95**: 20133–20146. doi:10.1029/JB095iB12p20133.

Wyld, S.J., Umhoefer, P.J., and Wright, J.E. 2006. Reconstructing northern Cordilleran terranes along known Cretaceous and Cenozoic strike-slip faults: Implications for the Baja British Columbia Hypothesis and other models. *In* Paleogeography of the North American Cordillera: Evidence For and Against Large-Scale Displacements. *Edited by* J.W. Haggart, R.J. Enkin, and J.W.H. Monger. Geological Association of Canada Special Paper, **46**: 227–298.

Wynne, P.J., Irving, E., Maxson, J.A., and Kleinspehn, K.L. 1995. Paleomagnetism of the Upper Cretaceous strata of Mount Tatlow: Evidence for 3000 km of northward displacement of the eastern Coast Belt, British Columbia. Journal of Geophysical Research, **100**: 6073–6091. doi:10.1029/94JB02643.